

NETHERLANDS GEODETIC COMMISSION
PUBLICATIONS ON GEODESY
VOLUME 5

NEW SERIES
NUMBER 3

DELFT UNIVERSITY EQUIPMENT
FOR PHOTOGRAPHIC
SATELLITE OBSERVATIONS

by

T. J. POELSTRA and F. W. ZEEMAN
Geodetic Institute, Delft University of Technology

1974
RIJKSCOMMISSIE VOOR GEODESIE, KANAALWEG 4, NETHERLANDS

PRINTED IN THE NETHERLANDS BY W. D. MEINEMA B.V., DELFT

ISBN 90 6132 220 0

CONTENTS

Summary	4
1 Introduction	5
2 Camera TA-120	8
2.1 General	8
2.2 Main shutter	9
2.3 Tracking power	10
2.4 Focal-plane chopper	14
2.5 Calibration	24
2.6 Operation	25
2.7 Signal-processing	26
3 Camera K-50	27
3.1 General	27
3.2 Main shutter	32
3.3 Tracking power	32
3.4 Focal-plane chopper	32
3.5 Calibration	34
3.6 Operation	34
4 Mounting	36
4.1 General	36
4.2 Polar- and declination axis	36
4.3 Driving system	37
5 Time-keeping	45
5.1 Time measurements	45
5.2 Time-keeping equipment	45
5.3 Portable quartz clock	47
6 Time recorders	51
6.1 Time recorder with printed output	51
6.2 Time recorder with punched output	56
7 Annexes	58
7.1 Some tables with relation to the TA-120 chopper	58
7.2 Nomogram "revolutions per minute" of the chopper motor	60
7.3 Calibration	60
7.4 Basic design data for the K-50 chopper	64

SUMMARY

In 1966, following some years of preparation, the Delft Working Group for Satellite Geodesy started photographic observations of satellites. Since then the camera station of the Geodetic Institute of Delft University of Technology has continued participating in internationally coordinated geodetic satellite observation programmes. Contributions were made to the Western European Satellite Triangulation Programme (WEST), the National Geodetic Satellites Programme (NGSP), the International Satellite Geodesy Experiment (ISAGEX), and a Short Arc observation programme. Both optically passive and optically active satellites were observed. In 1969 the station was relocated, but still it remained in the vicinity of Delft until definitive re-establishment followed in 1973 at a more suitable site near Apeldoorn. This publication concentrates in particular on the equipment of the camera station; this consists, inter alia, of two cameras, TA-120 and K-50. The TA-120 has been purchased from N.V. Optische Industrie "De Oude Delft" and is of the concentric Bouwers-Maksutov mirror type; the K-50 camera is a geodetic satellite camera designed on the basis of a K-50 lens-cone assembly. This camera is equipped with an automatic reloading device, capable of holding eight photographic plates (size 8" × 10"). Time is obtained by means of a revolving focal-plane chopper. These two cameras are mounted together in an equatorial Dutch mounting. This mounting is automatically positioned using predictions on punched cards. Time is recorded on punched tape and print, time-keeping is done by means of a rubidium-frequency standard.

The K-50 modification, the equatorial mounting partially and the time-recording equipment were designed and constructed at Delft University workshop. The authors are much indebted to all those who contributed to this project.

1 INTRODUCTION

When photographing an artificial earth satellite, simultaneously from different places on earth at mutual distances of some hundreds to some thousands of kilometres, one obtains in principle a number of photographic images of the satellite projected against a background of stars. A specific star catalogue with known directions to certain selected stars, yields a bundle of directions per satellite image: from every participating station one direction that goes through one particular point, namely the satellite. Repetition of this simultaneous photographing, from the same places on earth, gives again a number of directions all going through one point in space etc. etc. Each two of these directions defines a plane; these planes intersect; the directions of the intersection lines represent the mutual direction between all observing sites. In this way all mutual directions between all observing sites can be determined, entirely geometrically, not taking account of gravity.

In brief, this is a technique for measuring a number of directions to a corresponding number of satellite positions in space, from different locations at particular moments. Since the geometry of such a network has to be well determined and taking into consideration the height of most of the available satellites, the necessary distance between the locations is rather large. This implies international aspects and also the possibility of world-wide applications.

Because of the fact that the Delft equipment was developed for this particular technique, other techniques such as reconstruction of satellite orbits for gravity purposes are beyond the scope of this paper.

For reasons of accuracy the directions are being determined by means of photographing the projections of a part of the satellite orbit on the celestial sphere; time should be recorded on marked places in this photographic trail, since for computational reasons the orientations of the earth with regard to the celestial sphere must be known; time-recording is also needed to achieve a sufficiently accurate (artificial) simultaneousness.

Two types of geodetic satellites are available for this geometric method of satellite-observations: optically passive and optically active ones. The first type, the passive one, reflects the incoming sunlight. The shape is mostly spherical with a diameter of about 5 to 40 metres. The second type, the active one, has an onboard flashing beacon.

Irrespective of whether the satellite observed is of the active type or of the passive type, the measured directions and moments must comply with certain standards of accuracy.

In the event that the accuracy of the satellite triangulations should equal the accuracy of existing classical, continental, triangulations, then:

$$1 \times 10^{-5} > \frac{\Delta l}{l} > 1 \times 10^{-6} \dots \dots \dots (1.1)$$

In (1.1) Δl is the radius of the supposedly spherical relative standard surface that represents the relative precision of the coordinates of any two points of a system; l is the distance between these two points.

Accepting a level of proportional precision of 1×10^{-6} and supposing that the distance l and the height are of the same order of magnitude, means a level of precision for the measurement of the directions of 0.2 second of arc. The following matched specifications apply for the time-recording:

Table 1

height (km)	speed (km/s)	Δl (m)	requirement Δt (ms)
600	7.3	0.6	0.1
1100	7.2	1.1	0.2
1600	7.1	1.6	0.2
2100	6.9	2.1	0.3
2600	6.6	2.6	0.4
3100	6.4	3.1	0.5
3600	6.3	3.6	0.6

In practice, these requirements are being used as guide numbers for the standard deviations of the separate stochastic quantities, that appear in parts of the total equipment, measurements and computing process. The accuracy of the directions (α , δ), expressed in terms of right ascension and declination, and time-recordings (t) is a function of the accuracy of a number of such stochastic quantities.

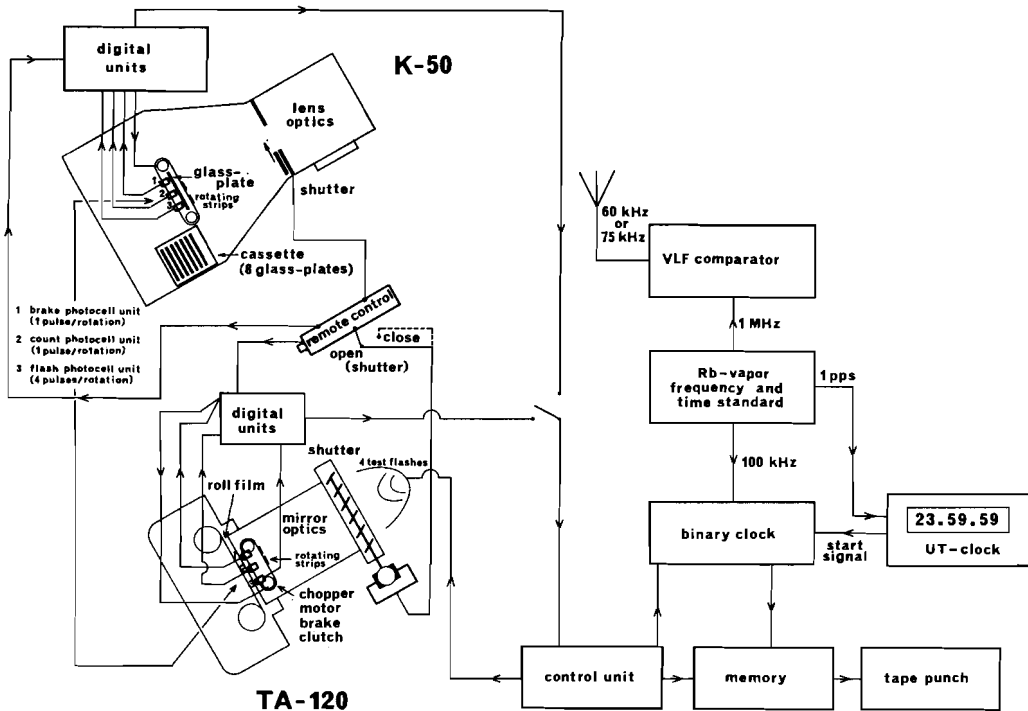


Fig. 1. View of the complete set-up.

The directions and time-recordings are determined by means of an equipment unit as shown in Fig. 1. This consists of:

- a Bouwers-Maksutov concentric-mirror type camera TA-120, made by N.V. Optische Industrie "De Oude Delft"; $F = 1200$ mm, $D_{\text{eff}} = 210$ mm, field of view $5^\circ \times 5^\circ$, using film;
- a lens type camera K-50; this camera has been designed on the basis of a K-50 lens cone assembly, $F = 900$ mm, $D_{\text{eff}} = 300$ mm, field of view $10^\circ \times 15^\circ$, using $8'' \times 10''$ glass plates;
- an equatorial mounting with punched card positioning, partially manufactured by Rademakers N.V., Rotterdam. This so-called minimount permits dual mounting of the two cameras;
- time-recording equipment, recording on punched paper tape, suitable for the focal-plane choppers of both cameras; printed output is also possible. Time-resolution $\approx 100 \mu\text{s}$;
- electronic control equipment, indication, power supplies;
- a Hewlett-Packard rubidium-frequency standard for frequency- and time-keeping purposes;
- radio receivers for reception and comparison of radio frequencies and time signals;
- a Mann 422 F monocomparator for measuring x - en y -coordinates on the photographic plates;
- additional facilities.

Some aspects of this equipment are dealt with in the following chapters.

2 CAMERA TA-120

2.1 General

This camera (Fig. 2) has a focal distance of $F = 1200$ mm, the diameter of the entrance-pupil being $D = 300$ mm; the relative effective aperture amounts to approximately $f/6$. The field of view is $5^\circ \times 5^\circ$, the optical system consists of a number of Bouwers-Maksutov concentric spherical mirrors. Though the field of view is rather limited, the image quality is very good. Moreover, there is the large "scale" of 1 second of arc corresponding to $6 \mu\text{m}$.

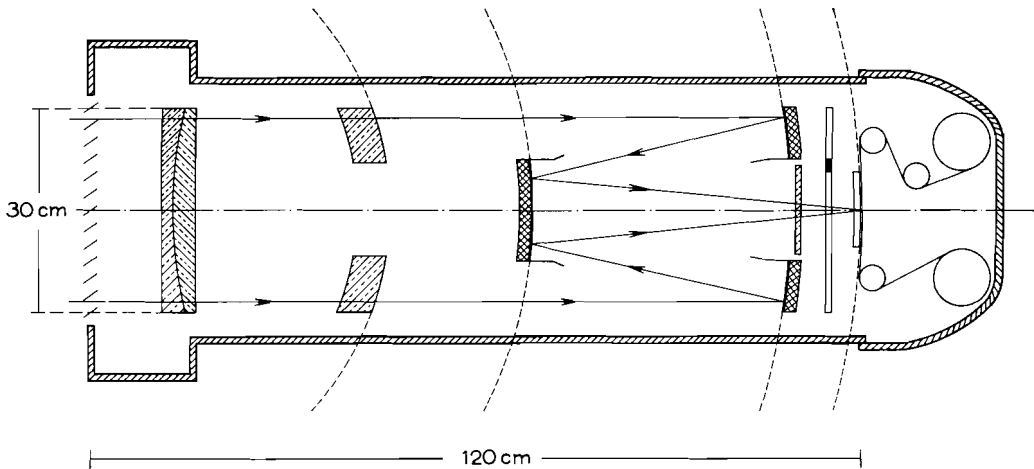


Fig. 2. Cross-section of TA-120 camera. The camera has been designed by N.V. Optische Industrie "De Oude Delft", at Delft, in accordance with the Bouwers-Maksutov principle, $F = 120$ cm, $D = 30$ cm.

The image plane is spherically shaped inherent to the optical system. This means that only film can be used. This film is contained in a cassette and can be transported automatically, offering the great advantage of a short reloading-time. All optical surfaces are spherical with a common centre of curvature positioned in the centre of the entrance-pupil. Each line passing through this centre can be seen as an optical axis. Therefore, there is no coma and no distortion and the image quality should be uniform over the entire field. The latter conclusion, however, is probably not valid, since the film is pressed on to the curved (convex) image plane. This procedure may cause undesirable film-deformation which may contribute to the final determination of the station-to-satellite directions. When determining the directions between the station and a number of satellite positions, the method of the linear plate constants (Turner) is applied within a surface on the film corresponding to approx. $1^\circ \times 1^\circ$. The effect of the linear part of the film deformation is thus eliminated. The

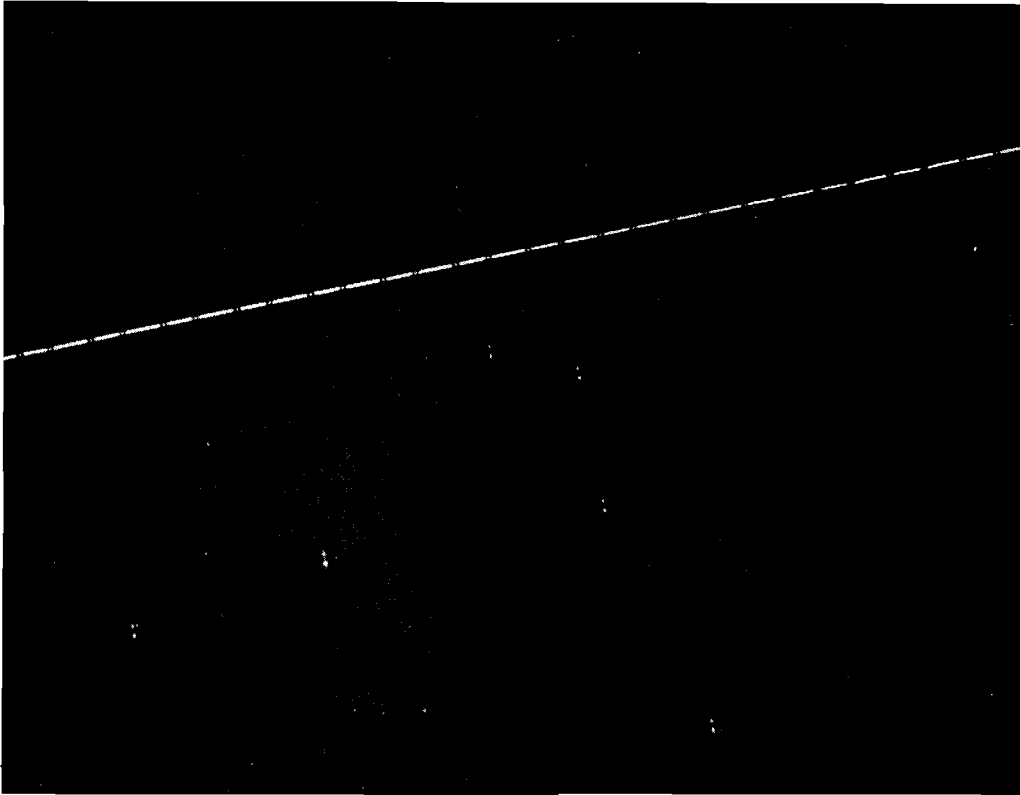


Fig. 3. Enlargement of a record of the (passive) Pageos satellite, made 17 April 1969. The markings in the track have been made by a chopper, during the exposure. The star-images have been produced twice to make them easily recognizable. The images with the largest diameter of each pair belong to the proper exposure.

effect of a possible non-linear part of the film deformation is estimated to contribute less than $1''$ to the standard deviation of one single direction of the station to a satellite position. The camera is suspended in a mounting, the so-called "Minimount".

This equatorial mounting compensates for the rotation of the earth; in the case of good exposures (Fig. 3) measurable images with diameters of 25 microns, corresponding to $\pm 4''$, have been obtained. Mounting and camera have been installed in a housing at Ypenburg airfield, which housing could be moved in two directions. At present the equipment is installed in the new Kootwijk observatory (Fig. 4).

2.2 Main shutter

The main shutter (Fig. 2) has been constructed in the University workshops and may be described as a "louvered"-type shutter. The somewhat bent blades have bearings on both sides. Driving is effected via handles all of which are actuated by one driving-lever. The latter is controlled by a 24 V DC electro-magnet. When the shutter must be opened, this magnet

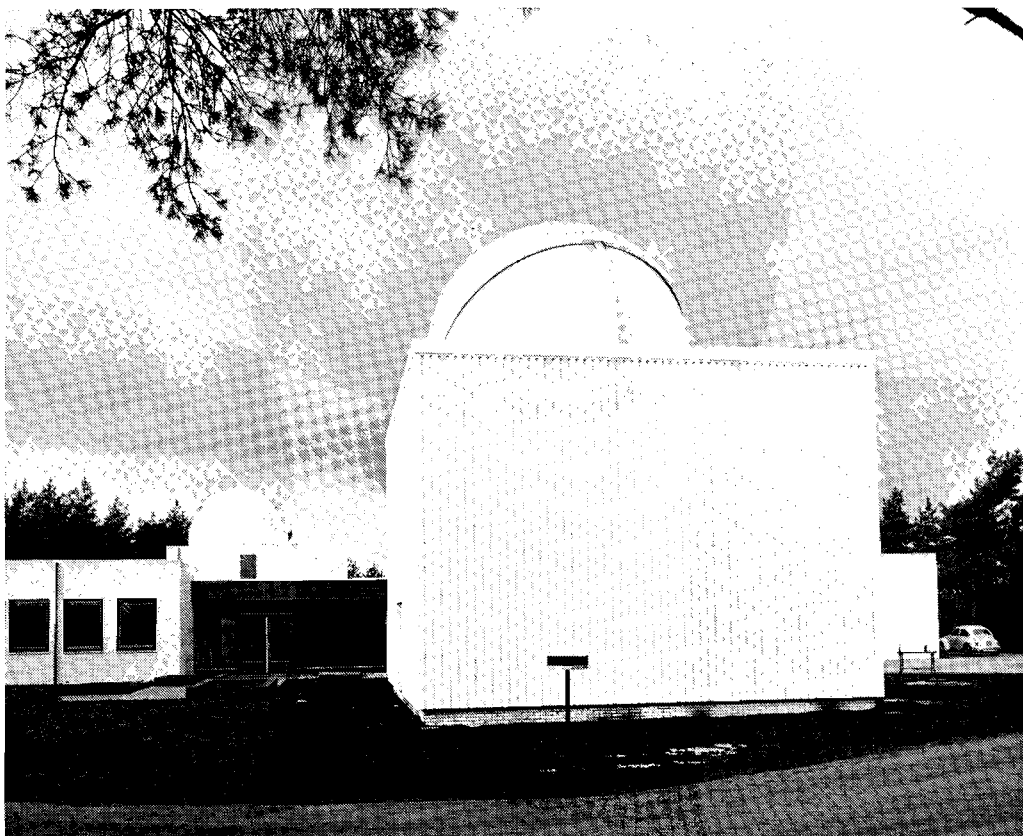


Fig. 4. The new Kootwijk observatory.

receives an energizing voltage; if the shutter blades are in the correct position (defined by micro-switches), then the magnet receives a lower hold current. Additional diaphragms can be placed in front of the main shutter.

2.3 Tracking power

A good photograph shows:

1. a satellite track;
2. a number of reference stars, forming a known matrix of directions on which the direction to the satellite is measured out;
3. a foggy background owing to the brightness of the sky.

At a certain moment during the exposure there is a distribution of intensity in the image plane. When this distribution of intensity is integrated in the time, it will result in a distribution of exposure which is converted into a distribution of density by the photographic process.

Disregarding the background fog (theoretically incorrect, but, in practice, permissible in

most cases), it may be said that the satellite has been successfully photographed, if the density in the processed satellite track has exceeded a certain threshold value. Dependent on emulsion and processing method, this is the case if the exposure (L_s) has exceeded a certain minimum value (L_{min}). For sensitive emulsions (e.g. Kodak Tri-X) and appropriate processing this threshold value is $L_{min} = 10^{-2}$ to 10^{-3} lx.s.

The condition for satellite photography will be:

$$E_s \geq \frac{\omega F d}{\tau D^2} \cdot L_{min} \dots \dots \dots (2.3.1)$$

in which:

- E_s = intensity of illumination by the satellite at the position of the camera in a plane perpendicular to the direction to the satellite
- D = diameter entrance-pupil camera
- F = focal distance
- ω = angular speed of the satellite image over the emulsion
- d = effective diameter of the satellite image (it is assumed that the intensity of illumination inside this diameter is uniform); representative value for quality optics: 25 μ m
- τ = transmittance factor of the camera optics (dependent on construction and quality).

From (2.3.1):

$$\log E_s \geq \log \left(\frac{\omega F d}{\tau D^2} \cdot L_{min} \right)$$

$$-2.5 \log E_s - 14.2 \leq -2.5 \log \left(\frac{\omega F d}{\tau D^2} \cdot L_{min} \right) - 14.2 \dots \dots \dots (2.3.1a)$$

In astronomy one does not use the intensity of illumination E by a star but one uses magnitude m , related to E by:

$$m = -2.5 \log E - 14.2$$

analogous for satellites:

$$m_s = -2.5 \log E_s - 14.2 \dots \dots \dots (2.3.2)$$

For most satellites m_s is never a constant as with most stars. For instance, for Pageos m_s ranges from +3 to +6 (dependent on satellite range, satellite elevation and position of the sun).

(2.3.1a) and (2.3.2) yield:

$$m_{s(max)} = -2.5 \log \left(\frac{\omega F d}{\tau D^2} \cdot L_{min} \right) - 14.2$$

or:

$$P = m_{s(\max)} + 2.5 \log \omega = 2.5 \log \left(\frac{\tau D^2}{F d \cdot L_{\min}} \right) - 14.2$$

Or, with ω in $^\circ/s \approx 1/60$ rad/s, it can be found that:

$$P = m_{s(\max)} + 2.5 \log \omega^\circ = 2.5 \log \left(\frac{\tau D^2}{F d \cdot L_{\min}} \right) - 9.8 \quad \dots \dots \dots (2.3.3)$$

P is the so-called “tracking power”, which thus appears to be the magnitude of a satellite, having a topocentric angular velocity of $1^\circ/s$, that can marginally be recorded. It is an optical photographic constant that characterizes the capability for photographing artificial satellites. Based on experimentally obtained values:

$$\left. \begin{aligned} L_{\min}(\text{Tri-X}) &\approx 5 \times 10^{-3} \text{ lx.s} \\ L_{\min}(2475) &\approx 1 \times 10^{-3} \text{ lx.s} \end{aligned} \right\} \dots \dots \dots (2.3.4)$$

it was experimentally found that:

$$\text{and } \left. \begin{aligned} P &= 4.1 \text{ (KODAK Tri-X)} \\ P &= 5.9 \text{ (KODAK 2475)} \end{aligned} \right\} \dots \dots \dots (2.3.5)$$

A few corresponding values calculated from (2.3.3) and (2.3.5) are shown in table 2.

Table 2

ω°	$m_{s(\max)}$	
	Tri-X	2475
1.0	4.1	5.9
0.9	4.2	6.0
0.8	4.3	6.2
0.7	4.5	6.3
0.6	4.7	6.5
0.5	4.9	6.6
0.4	5.1	6.9
0.3	5.4	7.2
0.2	5.9	7.7
0.1	6.6	8.4
0.05	7.4	9.1
0.01	9.1	10.9

As may be expected, the threshold magnitude $m_{s(\max)}$ increases with decreasing ω° . For a particular satellite path ω° can be reduced by:

1. turning the camera in the direction of movement of the satellite (Baker-Nunn camera);
2. displacing the plate or film during the exposure in the direction of satellite image motion; and
3. optically by influencing the light-path in the camera, by means of a rotating glass (Markowitz) for instance.

A similar theory can be set up for photographing the reference stars. In practice, however, a photograph of a satellite in itself shows sufficient reference stars. If necessary, the number of stars to be photographed may be increased by an equatorial camera set-up. As far as this is concerned, there is no sense in going further than $m = 9$ or 10, because stars of less brightness have not been catalogued sufficiently.

A number of experiments have been carried out for testing the theoretical values P . In this case a passing satellite was simulated by moving the camera at varying speeds and, then, checking which stars (or rather magnitudes) can still be seen in the pictures. The values found by this procedure turn out to be identical with the calculated values. Moreover, it can be seen from (2.3.3) that P and, at the same time, $m_{s(max)}$ may be influenced, for instance, by changing D , or by readjusting the diaphragm. This has been necessary in those cases, where Echo 1 and Echo 2 were photographed; a diaphragm is sometimes used when Pageos is photographed. These diaphragms can be slid in front of the main shutter and have concentrically cut rings which transmit the light.

Replacing D by VD , it follows from (2.3.3):

$$P' = 2.5 \log \frac{\tau D^2}{F d L_{min}} + 5 \log V - 9.8$$

or:

$$P' = P + 5 \log V \dots \dots \dots (2.3.6)$$

From (2.3.3) and (2.3.6):

$$m'_{s(max)} = m_{s(max)} + 5 \log V \dots \dots \dots (2.3.7)$$

In other words, when using the diaphragm, the values given in the table 2 are increased by $5 \log V$, as follows:

diaphragm (transmittance)	V	$5 \log V$
5%	0.05	-6.5
10%	0.10	-5.0
20%	0.20	-3.5
30%	0.33	-2.4
50%	0.50	-1.5

Finally, it must be mentioned, that the tracking power of a camera can be used only when photographing passive satellites. In the case of active satellites (Fig. 5), the following condition must be satisfied:

$$L_s = t \left(\frac{D}{d} \right)^2 E_s \geq L_{min} \dots \dots \dots (2.3.8)$$

in which t = exposure time (= duration of light impulse).

Here the values for L_{min} which have been found experimentally according to (2.3.4) can be used again.



Fig. 5. Enlargement of a record of the (active) Geos-2 satellite, made 5 April 1969. Three light-flashes are indicated. These are the dots to which the arrows point.

2.4 Focal-plane chopper

a. *General*

As described in chapter 1, the aim is to record directions as well as instants of time. In the case of an active satellite this is not difficult: the flashes are recorded photographically and the instants of time given by the central prediction centre, are sufficiently accurate, so the flash-moments are fixed exactly.

This is not so when passive satellites are to be photographed; during the photographic procedure two main recordings have to be made: the satellite track has to be chopped and the moments at which this is done recorded with sufficient accuracy (table 1).

The part required for this purpose the so-called chopper, Fig. 6, has been developed, manufactured and fitted in the workshop of the working group. A double strip of light-weight material moves in two planes, the important point being the movement in the plane nearest to the focus (a distance of approx. 15 mm). When the double strip is moving in this plane, the procedure is as follows: the beam of light which forms the satellite image (track) is consecutively chopped-transmitted-chopped, in other words there is a suppression of light, followed by a transmittance and, then, a suppression again, after which the light is trans-

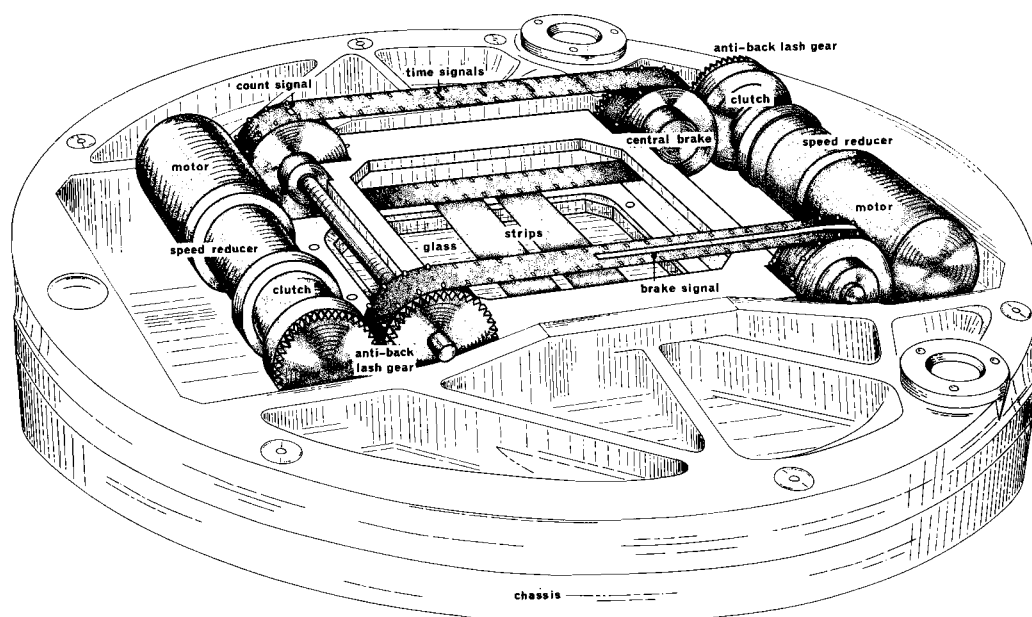


Fig. 6. Sketch of the chopper as it is positioned just in front of the image-plane in the removable rear-part of the camera.

mitted during a longer period until the procedure starts anew during the next cycle of the chopper.

The double strip is fitted to two driving-belts which are driven by means of sprocket-wheels. The latter wheels are driven by one of the two DC motors, dependent, inter alia, on the speed of the satellite to be observed. The motor to be used, is fed by a stabilized direct current; the number of revolutions of the driving motor and, at the same time, the frequency (speed) of the strip, are controlled by varying the voltage. So, the frequency of the (double) strip can be controlled in order to be able to adapt its speed to the topocentric angular-speed of the satellite, as follows:

Table 4

angular-speed of the satellite	strip frequency	linear speed of the strip
0.87°/s	6.2 c/s	2.60 m/s
0.42	3.1	1.30
0.27	2.0	0.80
0.20	1.5	0.60
—	—	—
—	—	—
—	—	—
0.05	0.4	0.16

The high linear speeds desired are a consequence of the relatively long focal distance of the camera and the mechanical limitations owing to the construction of the camera so that the chopper cannot chop the light beam within 15 mm from the focus. Registration of the

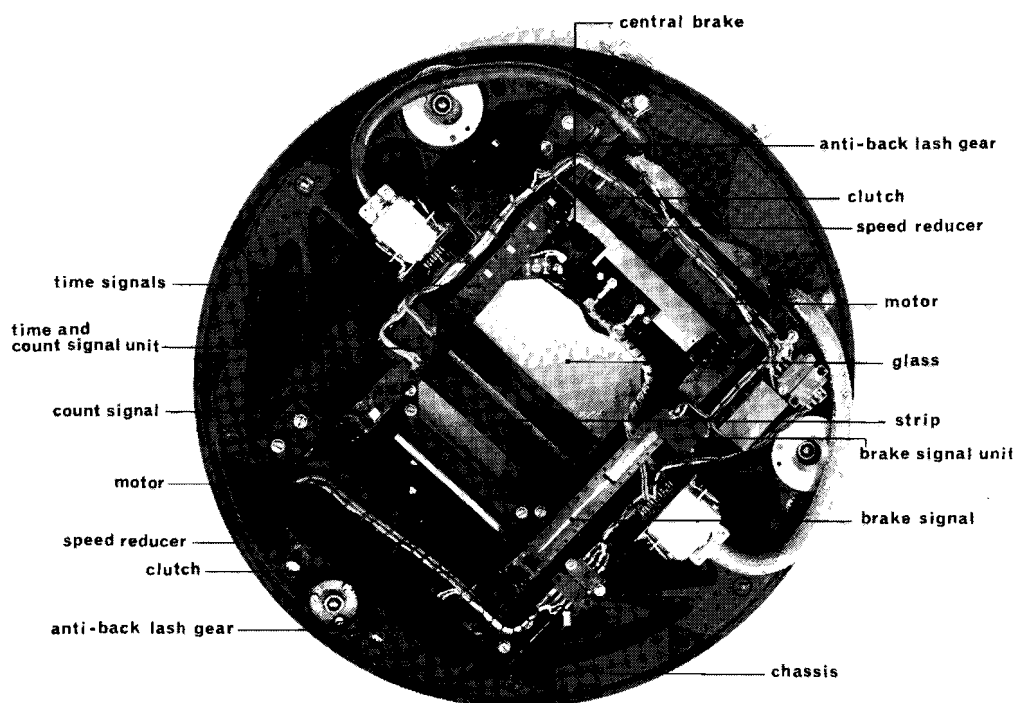


Fig. 7. Chopper, constructed in the workshop of the working group.

moment at which the double strip produces the marks in the satellite track is not possible directly, but indirectly. For this purpose a number of pulses are generated each time the strip passes the field of view (Fig. 6: in this figure the rear part of the camera, i.e. the image plane has been drawn horizontally):

- 4 ("flash") time pulses
- 1 counting pulse
- 1 decelerating pulse

The flash- or time-pulses have two functions:

1. Each time the strip passes the field of view, these pulses can be used to trigger a stroboscope photo-electrically, each flash corresponding to one (fixed) position of the strip. By "position of the strip" is meant the situation of a line in the focal plane, which line, related to the fiducial marks, is the geometrical locus of all points, where a satellite track could have been interrupted at the moment that the coupled trigger-pulse actuates the stroboscope. There are four such lines and their position with respect to the fiducial marks can be determined by means of a special calibration recording. Such a calibration can be seen as reliable for a rather long time.
2. During the actual satellite recording the time instants of the pulses are registered on a punched tape, the chopper being started and stopped when the satellite is just in view or has almost disappeared out of view. During this procedure a small tracking telescope is

used in which the field of view of the camera has been indicated as an illuminated frame. By means of these recordings + registrations and a calibration recording, the instants of time of a number of selected choppings can be related to the local time-standard, via an interpolation procedure (for instance, a 2nd degree relation between strip coordinate x and instant t of the calibration). Furthermore, standard techniques are in use for synchronizing the local time-standard, for instance, by means of "HBG" time signals.

The counting- and braking pulses are generated in order to achieve that:

1. The strip always returns to the same zero(starting)-position.
2. The strip always makes a multiple of four revolutions.

For the sake of simplicity, photocells, lamps and the electronic equipment have not been indicated in Fig. 6. For these parts see Fig. 7.

b. Requirements for a chopper-motor

As indicated in table 1 there are stringent precision requirements for both the directions between station and satellite and the relative instants of time. With respect to the former requirement, this can be met by proceeding carefully during and after the exposure: stable camera pointing within $1''$ during a maximum of 5 minutes of exposure and, afterwards, careful processing; use of a plate-measuring apparatus (monocomparator) which enables standard deviations of 1 to $2 \mu\text{m}$ ($\approx 0.''2$ to $0.''3$) to be made in one single coordinate-reading. With respect to the accuracy of the instants of time registered, much depends on the chopper and, particularly on the accuracy of the running motors each time the strip passes through the field of view.

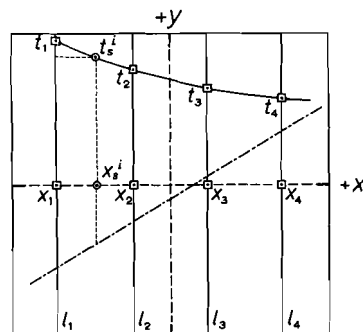


Fig. 8. Two exposures, superimposed via the fiducial marks. One exposure shows a satellite and stars, the other is a calibration picture showing four calibration lines l_1 through l_4 . Via the four pairs (x, t) , a second-degree curve, for instance, can be determined, as indicated here. t_s^i results then from the x_s^i .

In Fig. 8 a satellite exposure and an exposure of the four calibration lines are supposed to be superimposed via the fiducial marks system. So one group t_1 through t_4 corresponds to each point in the satellite track; the calibration coordinates x_1 through x_4 correspond to the group (the direction of rotation of the strip is parallel to the x -axis, the centre line of the double strip is parallel to the y -axis). So there are always 4 pairs (x, t) for each

passage of the strip: (x_1^i, t_1^i) to (x_4^i, t_4^i) , this being just sufficient to fit an overdetermined second degree curve $t^i = t^i(x)^i$ or $x^i = x^i(t^i)$.

With the aid of the x_s^i corresponding to a certain passage of the strip, the instant t^i can be found. The requirements Δt indicated in table 1 are the precision requirements for these (interpolated) points in the satellite track.

In the hypothetical case of an infinite number of calibration lines, the behaviour of the strip during while passing through the field of view could be fully reconstructed even in the case of a continuously varying speed of the driving motor, so that the requirements could always be met. For practical reasons, however, it was necessary to confine ourselves to four calibration lines and that makes the checking more difficult. The reason is that the interval between two time registrations renders possible uncontrolled behaviour. To compensate for this, at least for a part, the following procedure can be adopted: When the chopper operates (at a certain speed) three intervals per cycle can be computed:

$$t_2^i - t_1^i; t_3^i - t_2^i; t_4^i - t_3^i \text{ etc.}$$

With:

$$t_i = t_2^i - t_1^i \text{ (for instance)}$$

it follows from the application of the law of propagation of variations for normally distributed quantities that:

$$\begin{aligned} \overline{t_i, t_i} &= \overline{(t_2^i - t_1^i), (t_2^i - t_1^i)} \\ &= \overline{t_2^i, t_2^i} - \overline{t_1^i, t_2^i} - \overline{t_2^i, t_1^i} + \overline{t_1^i, t_1^i} \end{aligned}$$

With:

$$\overline{t_1^i, t_2^i} = \overline{t_2^i, t_1^i} = 0$$

and

$$\overline{t_2^i, t_2^i} = \overline{t_1^i, t_1^i} = \overline{t, t}$$

the result is:

$$\overline{t_i, t_i} = 2\overline{t, t}$$

or:

$$\Delta t_i = \Delta t \sqrt{2} \dots \dots \dots (2.4.1)$$

in which:

- Δt_i = standard deviation of an interval
- Δt = standard deviation of an instant.

The requirements for Δt indicated in table 1 can be converted via (2.4.1) into requirements Δt_i for the intervals t_i at a certain chopper speed.

When relating these Δt_i 's to their t_i 's for the various speeds, then the required relative precision for the number of revolutions of the driving motors is obtained:

$$\text{requirement} = \frac{\Delta t_i}{t_i} \approx 11.5\% \dots \dots \dots (2.4.2)$$

Since both Δt_i and t_i increase in a linear way in accordance with the increase of height for the various satellites, this requirement holds good for the whole control range of the driving motors.

Conversely, it follows from (2.4.1) that, if one gets an estimation of the standard deviations of the intervals, then it is possible to check whether the requirement (2.4.2) has been met, and this latter feature has been incorporated in the computer programme which evaluates the time-tapes from the tape punch. When the requirements are not met, the relevant registrations are rejected.

c. *The number of revolutions to be set*

Finally, a few remarks on the question of the speed of the chopper strip and its width in order to get easily measurable points in the satellite track during the recording of a certain

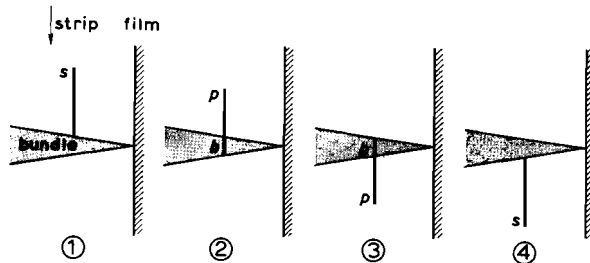


Fig. 9. Top-view, indicating how an interception is produced.

satellite. Fig. 9 shows a chopping procedure in four phases: one single strip (half the normal double strip) enters the beam, chops it, intercepts it and, then, allows it to pass through again. If a satellite track runs perpendicularly to the moving-direction of the strip, the following holds good:

$$\left. \begin{aligned} t_{ov} &= \frac{b}{v} = \frac{b}{OT} \\ t_{ond} &= \frac{p}{v} = \frac{p}{OT} \end{aligned} \right\} \dots \dots \dots (2.4.3)$$

in which:

- t_{ov} = time required for change-over from light to dark
- t_{ond} = time required for chopping
- b = local beam diameter in the plane parallel to the image plane
- s = width of the strip
- p = $s - b$
- O = circumference of the sprockets
- T = number of rotations per second of the sprockets
- v = linear speed of the strip.

A satellite with a height of approximately 500 km has a topocentric angular speed of about $0.8^\circ/s$, or on the film a linear speed of about 2 cm/s, when passing the zenith. If for instance an interruption is desired of $100 \mu\text{m}$ (good visibility is necessary for comparator measurements), this means:

$$t_{\text{ond}} = \frac{100 \mu\text{m}}{2 \times 10^4 \mu\text{m/s}} = 5 \text{ ms}$$

From (2.4.3) it then follows that: $p/v = 5 \text{ ms}$. If we now take $s \approx 10 \text{ mm}$ with $b \approx 5 \text{ mm}$ (and $p > b$), then $v = 1 \text{ m/s}$.

For practical reasons the following has been taken:

$$\text{in which: } \left. \begin{array}{l} s = 20 \text{ mm} \\ b = 5 \text{ mm} \end{array} \right\} \dots \dots \dots (2.4.4)$$

In the case of the lowest satellite being at a height of 500 km, this choice means a maximum v of 3 m/s. The displacement speed of the satellite (2 cm/s), therefore, is not even 1% of that of the strip.

If the strip moves in the same direction as the satellite, or in the opposite direction, there will be deviations in this order of magnitude. If we neglect these deviations then (2.4.3) holds good.

With:

$$v' = \frac{F\omega}{\varrho}$$

in which:

- v' = linear speed of the satellite image over the film
- ϱ = 1 radian in angle measurement

it results from (2.4.3) that:

$$\left. \begin{array}{l} L_{\text{ov}} = \frac{bF\omega}{OT\varrho} \\ L_{\text{ond}} = \frac{pF\omega}{OT\varrho} \end{array} \right\} \dots \dots \dots (2.4.5)$$

in which L_{ov} and L_{ond} respectively are the linear distance on the film of change-over from light to dark and chopping.

However, a sharpening of (2.4.5) is also necessary. When photographing a satellite of a magnitude which exceeds (rather much) the threshold-magnitude $m_{s(\text{max})}$, one, (e.g. the operator of the comparator) will interpret the total of a part of $2L_{\text{ov}}$ together with L_{ond} as an interception. In other words the real interception consists neither of L_{ond} only, nor of $L_{\text{ond}} + 2L_{\text{ov}}$, but it does consist of L_{ond} plus part of $2L_{\text{ov}}$. The question is, however, how large is this part.

To answer this question we assume that the outside of the light-beam which in the TA-120 images the satellite at a certain moment is bounded by a cone-mantle the image point of which is the cone-top; in connection with the position occupied by the second mirror inside the camera, we further assume the light-beam of the inside to be bounded also by a cone-mantle, the image point of which is again the cone-top. The imaging light is situated, then, between the two cone-mantles.

If we consider the case, in which the image point lies approximately in the centre of the image plane, then a cross-section is obtained in the plane of intersection, as indicated in Fig. 10. In this cross-section the light is situated between the two circles; we assume that the intensity of illumination is constant over the whole surface.

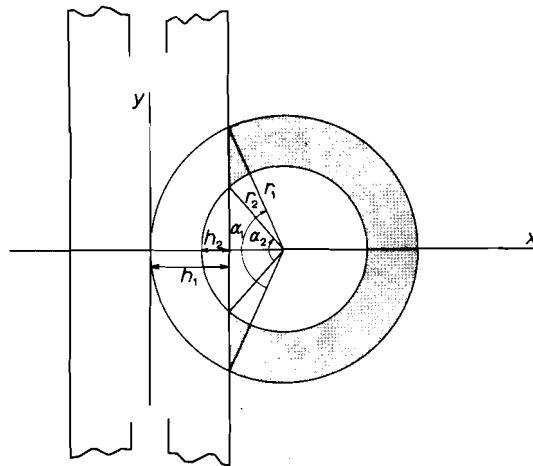


Fig. 10. Cross-section of a light-beam in the plane where the intercepting strips are moving nearest to the image plane. One of the strips is cutting the beam.

At a certain moment during the entrance of the strip into the beam, the surface of the segment, which seems to be cut already, is (see Fig. 10):

$$O_{\text{segment 1}} - O_{\text{segment 2}} = \pi r_1^2 \frac{\alpha_1}{360} - \frac{1}{2} r_1^2 \sin \alpha_1 - \pi r_2^2 \frac{\alpha_2}{360} + \frac{1}{2} r_2^2 \sin \alpha_2 \dots \quad (2.4.6)$$

with:

$$\cos \frac{1}{2} \alpha = 1 - \frac{h}{r}$$

In (2.4.6) we consider h to be an independent variable and $(O_{\text{segment 1}} - O_{\text{segment 2}})$ a dependent variable; this indicates the connection between the distance h the strip has covered in the beam and the total light quantity transmitted or intercepted (because this is directly proportional to $O_{\text{segment 1}} - O_{\text{segment 2}}$).

Therefore:

$$\left. \begin{aligned} \frac{h_1}{2r_1} = q &= f^1 \left(\frac{O_{\text{segm } 1} - O_{\text{segm } 2}}{O_1 - O_2} \right) \\ &= f^2 \left(\frac{E'_s}{(E'_s)_{t=0} \stackrel{\text{per}}{=} W} \right) \end{aligned} \right\} \dots \dots \dots (2.4.7)$$

In (2.4.7) f^1 and f^2 are functions, E'_s is the intensity of illumination of the satellite image and $(E'_s)_{t=0}$ is the same, however, at the moment that the strip starts suppressing the beam. The following results from (2.4.7):

$$E'_s = W \cdot (E'_s)_{t=0} \dots \dots \dots (2.4.8)$$

The contribution of L_{ov} to L_{ond} starts as soon as E'_s attains a value at which the satellite is no longer imaged, in other words until the threshold-magnitude has been attained; from (2.4.8) and (2.3.2) it follows that:

$$m_{s(\text{max})} = m_s - 2.5 \log W \dots \dots \dots (2.4.9)$$

From (2.4.7) and (2.4.9) it follows that:

$$\frac{h_1}{2r_1} = q = f^3 \{ m_{s(\text{max})} - m_s = -2.5 \log W \} \dots \dots \dots (2.4.10)$$

In (2.4.7) and (2.4.10) there are in total three relations in which q has been expressed explicitly in other parameters via the functions f^1, f^2, f^3 . It is very difficult to find these functions, owing to the implicit character of (2.4.6).

Therefore, q is determined in another way: from $m_{s(\text{max})}$ and m_s via (2.4.10):

$$-2.5 \log W = m_{s(\text{max})} - m_s \rightarrow W$$

via (2.4.7):

$$\frac{O_{\text{segm } 1} - O_{\text{segm } 2}}{O_1 - O_2} = 1 - W \rightarrow O_{\text{segm } 1} - O_{\text{segm } 2}$$

via (2.4.6):

$$\rightarrow \alpha \rightarrow \frac{h}{r} \rightarrow q$$

In Annex 1 the connection between $\{m_{s(\text{max})} - m_s\}$ and q has been given for the TA-120 camera. q having been determined in this way, the part of L_{ov} that contributes to L_{ond} can be given, i.e.:

$$L_{\text{ov}} - qL_{\text{ov}} = (1 - q)L_{\text{ov}}$$

So the total linear distance of the interception is:

$$L_{\text{ond}} + 2(1 - q)L_{\text{ov}} \dots \dots \dots (2.4.11)$$

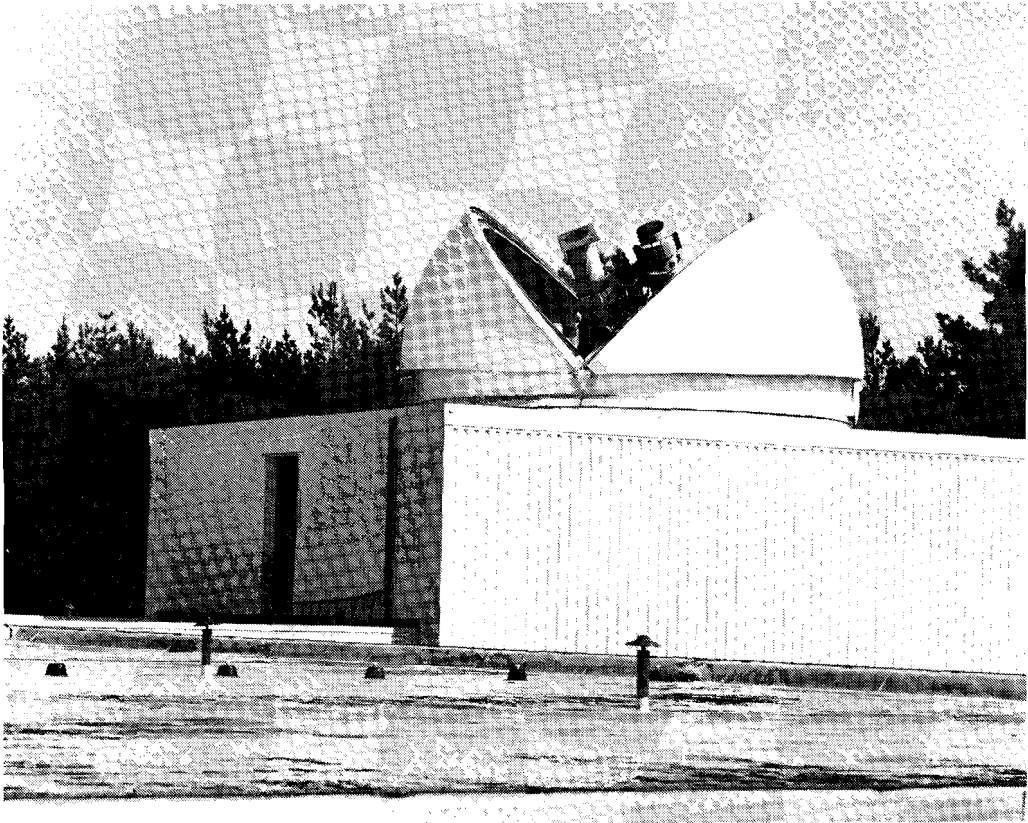


Fig. 12a. Camera-dome at Kootwijk with two cameras TA-120 and K-50 installed in it, suspended in one mount.

- ω = topocentric angular speed of the satellite in $^{\circ}/s$
 t = number of revolutions of the driving motor per minute
 q = ratio number, dependent on $\{m_{s(\max)} - m_s\}$.

With the aid of (2.4.15) a nomogram has been made, by means of which the number of revolutions of the chopper to be set can be found, taking as starting point the magnitudes given and to be predicted ($m_{s(\max)}$ and m_s respectively). The nomogram is given in Annex 2. The accuracy of the values of the figures given and found will be limited, taking into account the uncertainties of the magnitude prediction; the local atmospheric conditions may also differ greatly from those expected.

Further, it must be mentioned that practice has proved that, when using a double strip, there may be a kind of diaphragm effect. The values found for $m_{s(\max)}$, for instance, in table 2, must be increased as indicated in table 3, if one wishes to find the $m_{s(\max)}$ which shows measurable points in the track. The double strip having a slit-width of $s' = 10$ mm gives an additional diaphragm effect, in a way being identical with transmittance 50% in table 3.

2.5 Calibration

The calibration is meant to record the position of the calibration lines onto the film or

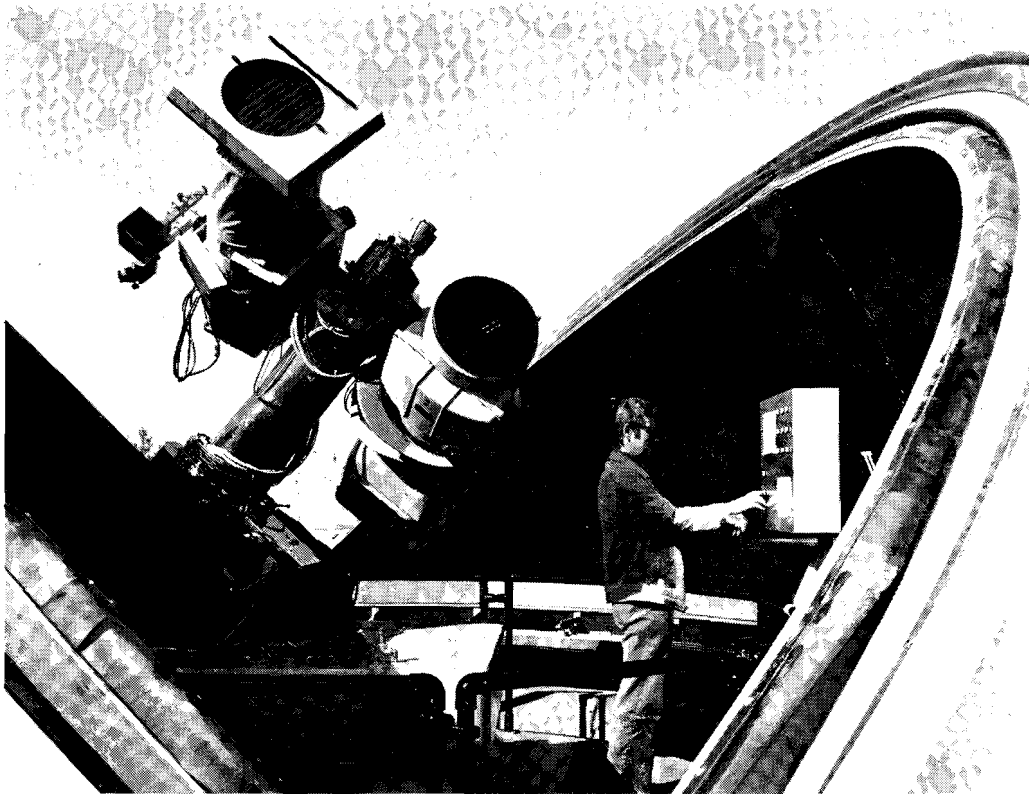


Fig. 12b. Close-up of cameras and mount.

plate. In the case of the TA-120 this is done by directing a flashlight into the camera; at the moments that the time-photocells deliver pulses, diffused light pulses enter into the camera and, consequently the shadows of the strip are recorded in four positions. The images of stars and satellite are all made via central projection through the projection centre. It seems logical also to produce the shadow during calibration, such that no corrections need be made to the calibration lines, considered the fact that the rotating strip does not move *in* the image plane, but *in front* of it. Annex 3 shows that the use of diffused light is sufficient for this purpose.

2.6 Operation

All camera and mount components are electrically driven. Push-button operation is, therefore, possible in the vicinity of the camera as well as in the installation room for the other equipment. The complete electronic unit has been installed in a separate room, in order to prevent extreme temperatures.

Main shutter

This is a louvered-type shutter positioned in front of the colour-correcting lens. The segments are rotatable on ball-bearings and are driven by means of a rotating magnet.

Film transport

The film cassette incorporates the driving device for the transport cycle. It consists of a film transport motor, a programme switch with motor and a plate which presses the film against the exposure frame. The starting-pulse effects the following cycle: releasing the pressure plate – transporting the film – pressing the pressure plate. During this cycle a counting-pulse is generated, which actuates the electronic film-counter. This counting-device indicates the number of unexposed frames in the cassette.

Fiducial marks

For the alignment of the exposures with respect to the calibration photographs, two fiducial marks are necessary. These are scratches on the glass plate in the image plane. They are illuminated by light-emitting diodes. The exposure is automatically controlled by the opening of the main shutter.

Chopper

The chopper unit in the camera has two motors (“fast and slow”), an electromagnetic coupling and brake. Switching into circuit in the correct order is effected by a relay-circuit. To give the strips the correct rotation speed as soon as possible, the motor is first brought to run at the correct speed, then the coupling is switched on and the brake is released.

The chopper makes a multiple of four rotations since this proved to be very practical for the evaluation of the exposures. Besides the four windows for time indications two extra windows have been made in the chopper tapes and the relevant extra lamp/photocell combinations have been fitted. The rotation of the chopper generates counting-pulses and decelerating pulses. The counting-pulses are worked out in a four-counter. The chopper stops:

- if the control-switch is released;
- and the counter is in the zero-position;
- and the braking-pulse has been received.

2.7 Signal-processing

- a. Three lamp/photodiode combinations have been fitted in the chopper by means of which combinations the windows in the transport-belt are scanned. The signals of the photodiodes are amplified in two-stage amplifiers fitted there. These amplifiers also provide matching to the 30 m coax-cables leading to the separate room where the registration equipment has been installed.
- b. The input of the equipment consists of Schmitt trigger-circuits, followed by a divider circuit. The speed of the chopper is determined by the speed of the satellite image on the film. The number of interceptions in the satellite track, however, is generally much larger than is interesting for further processing. Therefore, the possibility has been incorporated of limiting the number of time-registrations of interceptions. Each first, second, third or fourth interception can be registered, according to choice.

3 CAMERA K-50

3.1 General

The Delft K-50 camera (see Figs. 13 and 17) consists of three main parts:

- the optical assembly as purchased;
- the rear of the camera, as designed and constructed in the workshop of the working group;
- an adapter, combining the two parts and permitting the mounting of the camera.

The optical assembly has been designed by J. G. BAKER and constructed by the Perkin Elmer Corporation. The assembly includes seven lenses and has a flat field. The focal length is $F = 36''$ and the aperture $D = 12''$. The maximum effective field is 31° . After thorough consideration it was found that Kodak 103-F emulsion was the most suitable. The format of the glassplates was chosen to be $8'' \times 10''$, thickness $0.25''$, microflat (0.00002 inch/lin.inch). This reduces the effective field to $10^\circ \times 15^\circ$.

The plate reduction is achieved, according to a photogrammetric method, using central projection transformation formula's. The application of corrections for lens-distortion is part of this reduction process, i.e. the reduction-programme contains a determination of distortion-parameters.

The rear of the camera includes:

- a casted mantle with a removable rear part;
- a plate-changing mechanism capable of holding eight plates (Figs. 14, 16 and 17);
- a plate-holding and plate-pressure mechanism which adjusts every plate into its exact exposure-position and keeps it there during the exposure (Fig. 16);
- a calibration-unit;
- a focal-plane chopper (Fig. 15);
- control electronics.

The mantle is made of silumin, an aluminium-alloy. Dimensions haven been chosen such that the weight of the camera is limited. At a number of positions covers have been provided, to enable easy servicing.

The plate-changing mechanism consists of a cassette that must be placed in the cassette-holder (Fig. 14) and which was originally provided with a system of pressurized-air cylinders, oil cylinders and valves, which, together with a photo electric system cater for transporting and positioning the cassette. At the moment the air and oil cylinders have been replaced by an electric motor, driving a spindle.

When the cassette is in the correct position, a separate pressurized-air system pulls a glass-plate out of the cassette and presses it in the proper position, so that the emulsion lies in the image plane. When the exposure has been made, the glass-plate is transported back

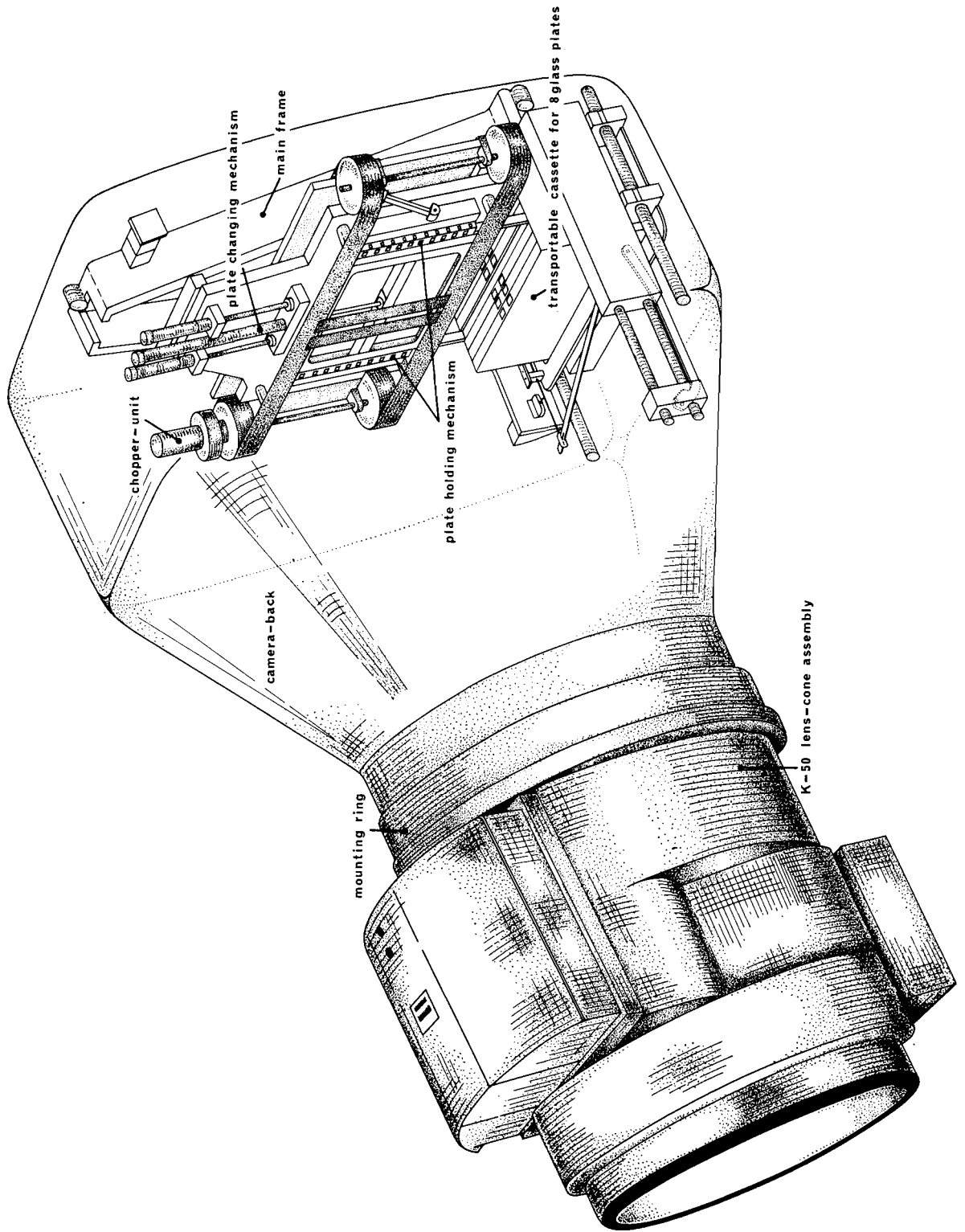


Fig. 13. Cut-away view through the K-50; principle-diagram.

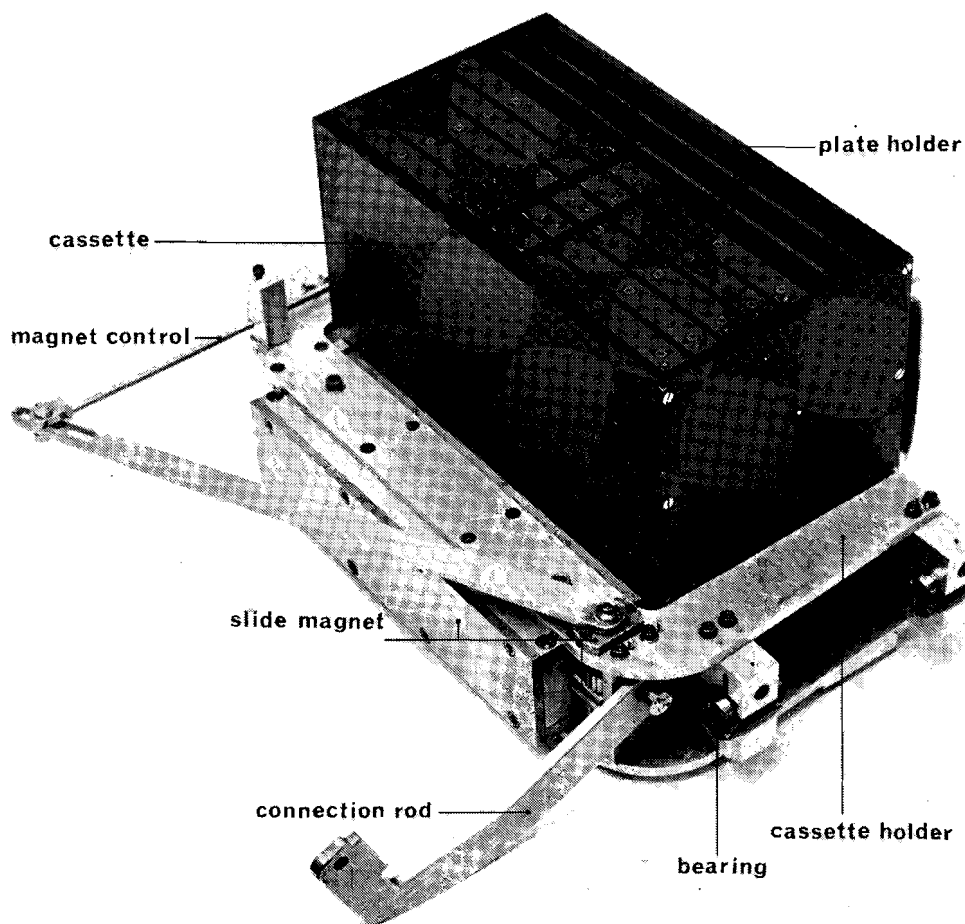


Fig. 14. Cassette of the K-50 and the cassette-holder.

into the cassette, after which the cassette is pushed one position upwards. Then the process can be repeated with the next glass-plate. In this way a short reloading time is achieved.

The rear of the camera has been designed with a view to two improvements in particular, based on the experiences with the TA-120 camera:

- a larger field. This was necessary with a view to future observations of laser satellites with the aid of the so-called illumination-laser;
- a flat field. This permits the use of glass plates and thus enables a greater accuracy in the reduction phase to be achieved.

The detailed design has been constructed almost completely in the workshop of the working group, after the various precision requirements had been formulated. The most critical part of the rear of the camera is the part containing the image plane, to which a focal plane chopper has been fitted permanently. Three fixing points have been provided for fitting the part to the camera.

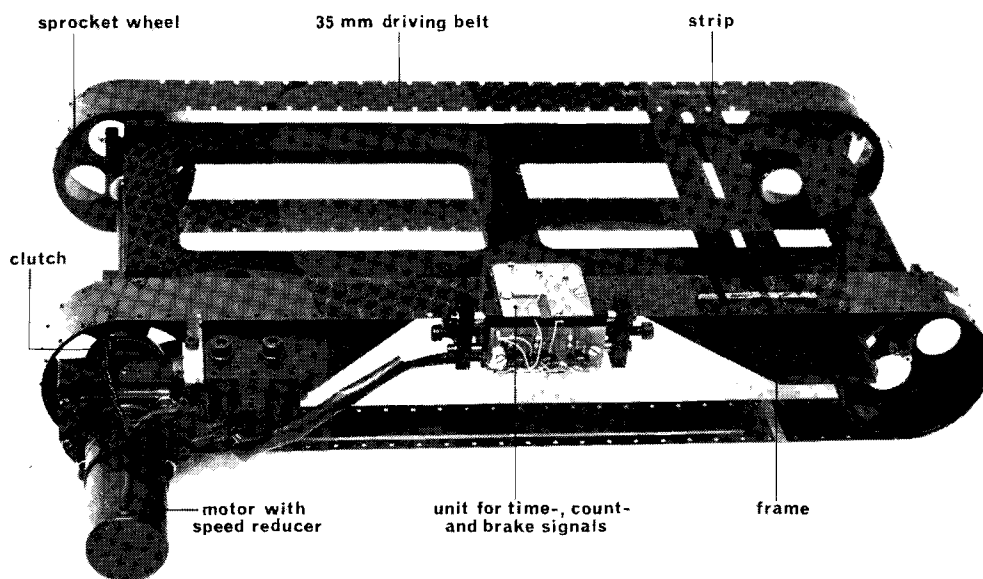


Fig. 15. Chopper of the K-50.

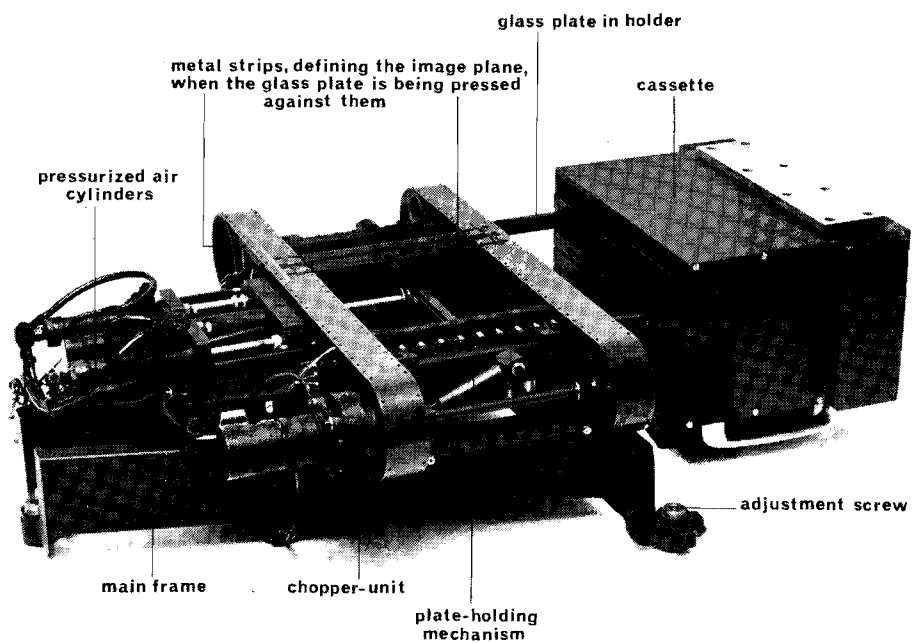


Fig. 16. Plate-holding unit and cassette unit of K-50 camera.

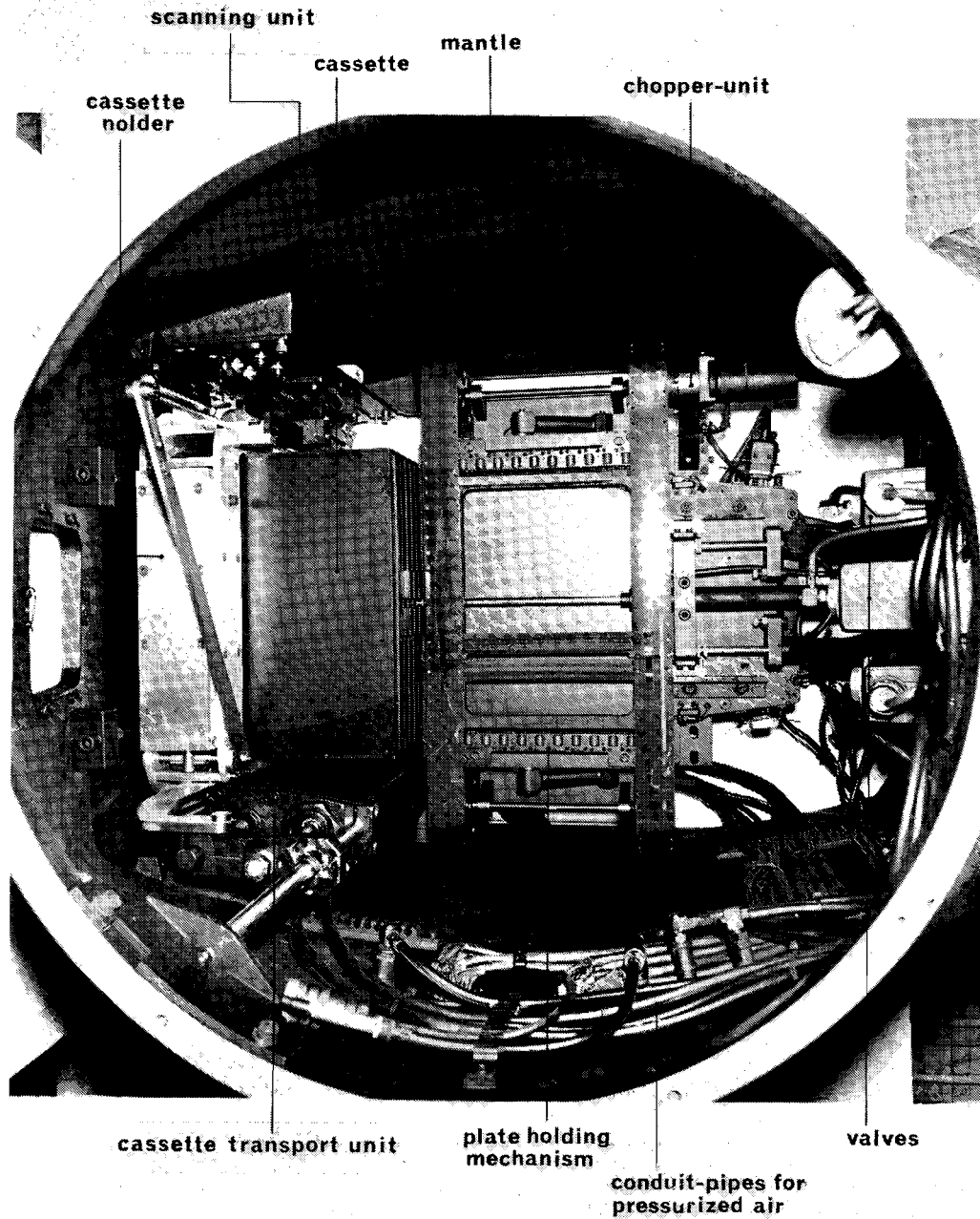


Fig. 17. Interior of the K-50 camera.

The distance between these points has been chosen such that the various requirements were met, for instance, with respect to the precision of adjustment of the image plane and the repeatability after assembly. Entering further into the design requirements is beyond the scope of this paper; these requirements have been set out in number of internal publications.

As regards the positioning of the cassette, the original system of air- and oil-cylinders has been replaced by a screw-spindle driven by an electromotor. The reason for doing this is that there were two drawbacks in the original system:

- the position of the cassette was not sufficiently accurate after transport;
- the system was sensitive to temperature, which resulted particularly in strongly varying transport times.

The K-50 camera has been fitted in the same equatorial mounting as the TA-120.

3.2 Main shutter

The main shutter has been fitted between the fourth and the fifth lens, at a position where the beam-diameter is smallest. The shutter consists in principle of a plate which either intercepts the beam or lets it pass through. The plate is slid in or out of the light-path, by means of an air cylinder. The speed is adjustable.

3.3 Tracking power

With the aid of (2.3.3) the value of the tracking power P can be calculated on the base of:

$$\begin{aligned}
 F &= 91.4 \text{ cm} \\
 D &= 30.5 \text{ cm} \\
 \tau &= 0.6 \\
 d &= 35 \text{ } \mu\text{m} \text{ (average)} \\
 L_{\min} &= (\text{KODAK 103-F}) = 7.9 \times 10^{-3} \text{ lx.s}
 \end{aligned}$$

It will then be found that:

$$P = \text{between } 3.5 \text{ and } 4.0$$

3.4 Focal-plane chopper

Just like the TA-120, the K-50 camera is equipped with a focal-plane chopper. The principle is identical, with the exception of the value of a few parameters. Moreover, this chopper with its double strip is able to pass over the emulsion at a shorter distance and on its way back it can pass behind the plate (Fig. 15). For the design of the chopper, the strip in the TA-120 has been taken as an example, i.e. the strip in the K-50 camera was to have the same maximum (linear) speed, because it enables satellites to be observed from distances down to 500 km. For constructional reasons, the following data were taken for the K-50 chopper:

Table 5

angular speed of the satellite	linear speed of the strip	strip frequency
0.87°/s	2.5 m/s	2.4 c/s
0.42	1.3	1.2
0.27	0.7	0.7
0.20	0.5	0.5
.		
.		
.		
0.05	0.2	0.2

The circumference of the driving belts is 106 cm, which is considerably more than the 42 cm in the TA-120. This gives a lower production of interceptions in the satellite track. In the evaluation practice of the TA-120 recordings it had been made a rule to skip interceptions systematically, so that this does not constitute a disadvantage.

Based on the field of view (of 10° × 15°) to be applied, and the plates to be used and the dimensions thereof (8'' × 10''), the interval lengths between the calibration lines are 60.0 mm. The following data can now be fixed:

Table 6

	TA-120	K-50
field of view used	4° 5' × 4° 5'	10° × 15°
length of interval	21.5 mm	60.0 mm
belt length	420 mm	1060 mm
circumference of sprocket <i>O</i>	120 mm	255.1 mm
max. speed of strip	2.6 m/s	2.5 m/s

The almost equal maximum linear speed, in combination with the greater distance (in the case of the K-50 camera) between the calibration lines, leads to more stringent requirements for the driving chopper motor, in the case of unchanged requirements for the accuracy of time marks to be registered. The required relative accuracy for the number of revolutions of the driving motor is (see (2.4.2) and the tables 1 and 14):

$$\text{requirement} = \frac{\Delta t_i}{t_i} \approx 3.9\% \dots \dots \dots (3.4.1)$$

Tests have proved that this requirement is met in certainly 90% of the observations.

In accordance with section 2.4 it can be found what is the connection between on the one hand, the number of revolutions of the motor per second and on the other hand, a number of camera-chopper and satellite parameters. Instead of (2.4.6), a simpler formula can now be used; in the case of the K-50 optics we assume that the imaging light-beam may be seen as one cone in which, per cross-section, the light intensity is constant. The following then holds good instead of (2.4.6):

$$O_{\text{segm}} = \pi r^2 \frac{\alpha}{360} - \frac{1}{2} r^2 \sin \alpha \quad \text{with} \quad \cos \frac{1}{2} \alpha = 1 - \frac{h}{r} \dots \dots \dots (3.4.2)$$

Based on (3.4.2), a table with q -values is calculated. It has turned out that these values deviate but slightly (1–2%) from the table of q -values for the TA-120, so that table 10 can be used also for the K-50.

With:

$$\begin{aligned} s' &= \text{slit width between the strips} = 6 \text{ mm} \\ b &= \text{local beam width} = 3 \text{ mm} \\ s' - b &= 3 \text{ mm} \\ F &= 91.4 \text{ cm} \\ O &= 25.5 \text{ cm} \end{aligned}$$

it follows from (2.4.13) that:

$$L_{bpt} = 60 \frac{\omega}{t} \{370q + 185\} \dots \dots \dots (3.4.3)$$

in which:

$$\begin{aligned} L_{bpt} &= \text{length of a point between two interceptions in the satellite track} \\ \omega &= \text{topocentric angular speed of the satellite in } ^\circ/\text{s} \\ t &= \text{number of revolutions of the driving motor} \\ q &= \text{ratio number, dependant on } \{m_{s(\text{max})} - m_s\} \end{aligned}$$

It has turned out that, within the existing uncertainties, the same nomogram can be used as for the TA-120, provided that the values found for t should be divided by 4.5. Furthermore, a comparison between the two systems can be made, with the aid of time registration tests and the tables 10, 13 and 14, so that, on the basis of the experience gained with TA-120 measurements, the settings for the K-50 can be found.

Finally, it can be mentioned that the focal-plane chopper will also be used in future for photographs made with the aid of the illumination laser, though not for the registration of times and interceptions in the satellite track, but for screening off the position on the photographic plate where the "light-echo" must be recorded. When firing the laser, diffusion phenomena are produced in the lower layers of the atmosphere and this light can be withheld by the strip, after which it is still possible to remove the strip so quickly that the light-pulse emanating from the satellite can be photographed.

The optical qualities of this camera and the reduction programmes to be used will be dealt with in future publications.

3.5 Calibration

The above-mentioned calibration lines are calibrated in the same manner as with the TA-120. Additional provisions have been made, however for each exposure to be provided automatically with calibration lines.

A periodical check must be made, however, to see that these lines all coincide with the real calibration lines, within the required limits.

3.6 Operation

Main shutter

This consists of a plate provided with a circular hole, which plate is moved by means of an air-cylinder. Operation is effected electrically with the aid of an electromagnetic valve.

Fiducial marks

These marks have been provided in a glass frame, luted to the window against which the photographic plate is pressed. They are illuminated with GaAsP diodes. A light-pulse is emitted automatically when the main shutter opens.

Chopper

The chopper is equipped with one motor and an electromagnetic clutch. The zero-position of the intercepting strips is outside the image plane, behind the photographic plate. This makes it possible for the chopper motor to attain the required speed smoothly or to decelerate smoothly in order to prevent vibrations as effectively as possible. The three chopper pulses are generated and used in the system in the same way as in the case of the TA-120.

Transport of photographic plates

From a mechanical and electrical point of view, transporting the plate-cassette in the camera, pulling out a plate and pressing it in the focal plane, are the complex features of the system. The cassette is transported by means of a screw-spindle driven by an electromotor. The transport is controlled by a photo-electric scanning unit, by means of which the eight pulling-out positions are fixed to within an accuracy of 0.2 mm. If the cassette is in one of these positions, a plate can be pulled out by a pneumatically moved rod and transported through a roller guide to the image plane. This cycle having been accomplished, the glass plate is pressed in the focal plane by means of an inflatable rubber membrane.

These three movements are controlled by a combined electronic and relay circuit incorporated in the rear cover of the camera. Since almost any incorrect movement will lead to mechanical damage, the control system is provided with every possible safeguard. Operation of the transport mechanism is effected with three push-buttons:

- START** – Transporting a plate from the cassette to the image plane. Pushing the button for the second time makes the plate move back into the cassette, after which the cassette moves one position. When the last position has been used the cassette moves back automatically into the initial position, after which it can easily be removed from the camera.
- PLATE RETURN** – Returning the plate from the focal plane to the cassette without the cassette shifting one position, should it be necessary to return an unexposed plate to the cassette.
- CASSETTE RETURN** – Returning the cassette to the initial position in the case where not all 8 plates in the cassette have been exposed, or if there are less than 8 plates in the cassette.

The control panel is provided with a number of pilot lamps and a plate-counter, by means of which the position of plates and cassette can be followed step by step.

4 MOUNTING

4.1 General

The mounting has been designed as a compact universal telescope mounting meeting professional requirements as generally specified for medium and large telescopes. Special attention has been given to the mechanical stability of the mounting and to an optimum accuracy for the setting of the coordinates and the sidereal tracking movement: during exposure of film and/or plate, the mounting compensates for earth-rotation with an accuracy of better than 0.''1 within 5 minutes of time.

Positioning is automatic with punched cards, or semi-automatic with thumb-wheel pre-selector switches. The coordinates hour angle t and declination δ are shown either on divided circles or on electronic digital displays. The information from the punched cards (predicted local-hour angle and declination) is fed into DC servo motors at the mounting; the required sign and amount of rotations are realized by means of subtracting-/adding-electronics and feed-back of incremental shaft encoders.

The aiming precision of the setting is $0^{\circ}.1$; the mechanical part of the mounting was constructed by Rademakers N.V., Rotterdam, in accordance with the design by B. G. HOOGHOUDT, Leiden. The positioning system has been designed and built in the workshops of the working group.

4.2 Polar- and declination axis

The housing consists of a lower part, adapted to the observatory latitude and floor height, and the upper part with a tubular extension for supporting the external polar axis. The top part of the polar axis rotates on a conical roller bearing, with a second bearing for preventing uplift.

The lower side is supported on a cylindrical bearing with a conical seat.

A preloading ring prevents backlash. Special precision bearings are used to assure a uniform motion with constant friction. The lower bearing centres the main wormgear, which is fixed permanently on the polar axis and driven by a worm with a springloaded anti-backlash system.

The lower part of the housing is welded and annealed. The upper part, tubular extension and polar axis are of high class castings. All parts have been overdimensioned to assure the rigidity of the mounting.

The lower part of the housing is bolted to a foot, embedded in a concrete pier. Provisions have been made for the adjustment of azimuth and polar height.

A two-part bearing house is bolted on top of the polar axis. Two special precision ball bearings support a short declination axis with a large internal diameter. The bearings are preloaded to prevent backlash. Each end of the declination axis contains a ring of threaded holes for mounting a telescope tube, camera or additional parts.

A wormgear is fixed centrally on the declination axis and driven by a worm with a

springloaded anti-backlash system. The worm-housing seals off the declination head. All parts are of high quality castings. The wall thickness and stiffeners have been chosen for adequate rigidity. The resulting deformations are negligible, taking into account the small dimensions.

4.3 Driving system

Fig. 18 shows schematically how the driving system for the camera mounting has been made up.

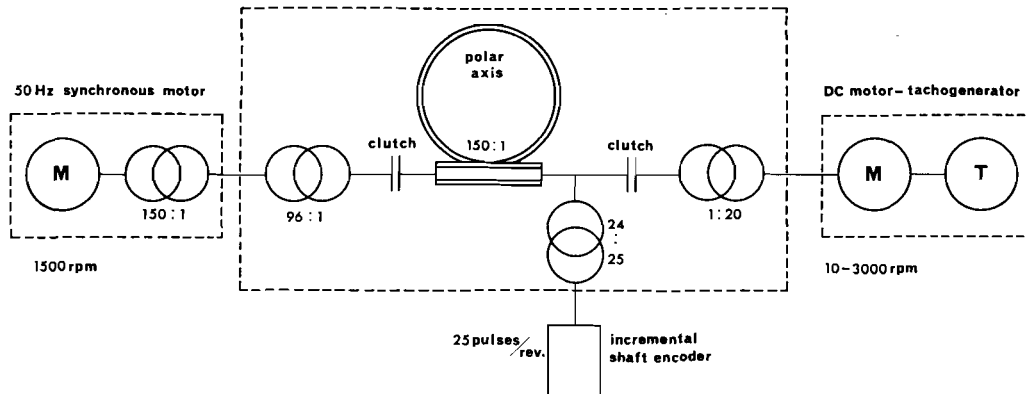


Fig. 18. Diagram of the "mini-mount" driving-system.

There are three external components:

- 50 Hz synchronous motor for sidereal tracking-movement
- Motor-tachogenerator combination for positioning
- Incremental shaft encoder for the automatic positioning system.

With the exception of the part for the sidereal tracking movement, the driving systems of both axes have been identically constructed.

Hereafter the following subjects will be dealt with in more detail:

- a. the sidereal tracking-movement
- b. the automatic positioning
- c. the motor driving.

a. Sidereal tracking movement

To compensate for the apparent movement of the stars with respect to the axis system of the mounting, it is necessary for the polar axis to make one revolution per sidereal day. This corresponds to a number of revolutions of $1/1440$ rev/sidereal minute.

Considering a normal 50 Hz synchronous motor with 1500 rev/min of solar time, a total retardation of $1500 \times 1440 = 2.160.000 = 150 \times 96 \times 150$ is necessary. The synchronous motor must be supplied with a frequency of 50 cycles per second of sidereal time. The ratio between solar and sidereal frequencies is 1:1.0027379. The correct supply-frequency should therefore be $50 \times 1.0027379 = 50.136895$ Hz. This value can be approximately achieved by dividing the 1 MHz signal of the frequency standard by 19945. This delivers a frequency of

50.137879 Hz. When feeding the motor with this frequency, a proportional tracking error of 0.02‰ will be made, corresponding to an angle error of $0.018 \cos \delta$ second of arc per minute of tracking.

b. *Automatic positioning*

Specifications: setting-range: 0.0– 399.9 (polar axis)
 –99.0– +99.0 (decl. axis)
 setting-accuracy: $0^\circ.1$
 data input: manual via thumb-wheel switches on two control panels.
 automatic via a punched-card reader
 output: via four output relays (three speeds and direction of rotation) to the motor control unit.

Principle of the operation (see block-diagram Fig. 19)

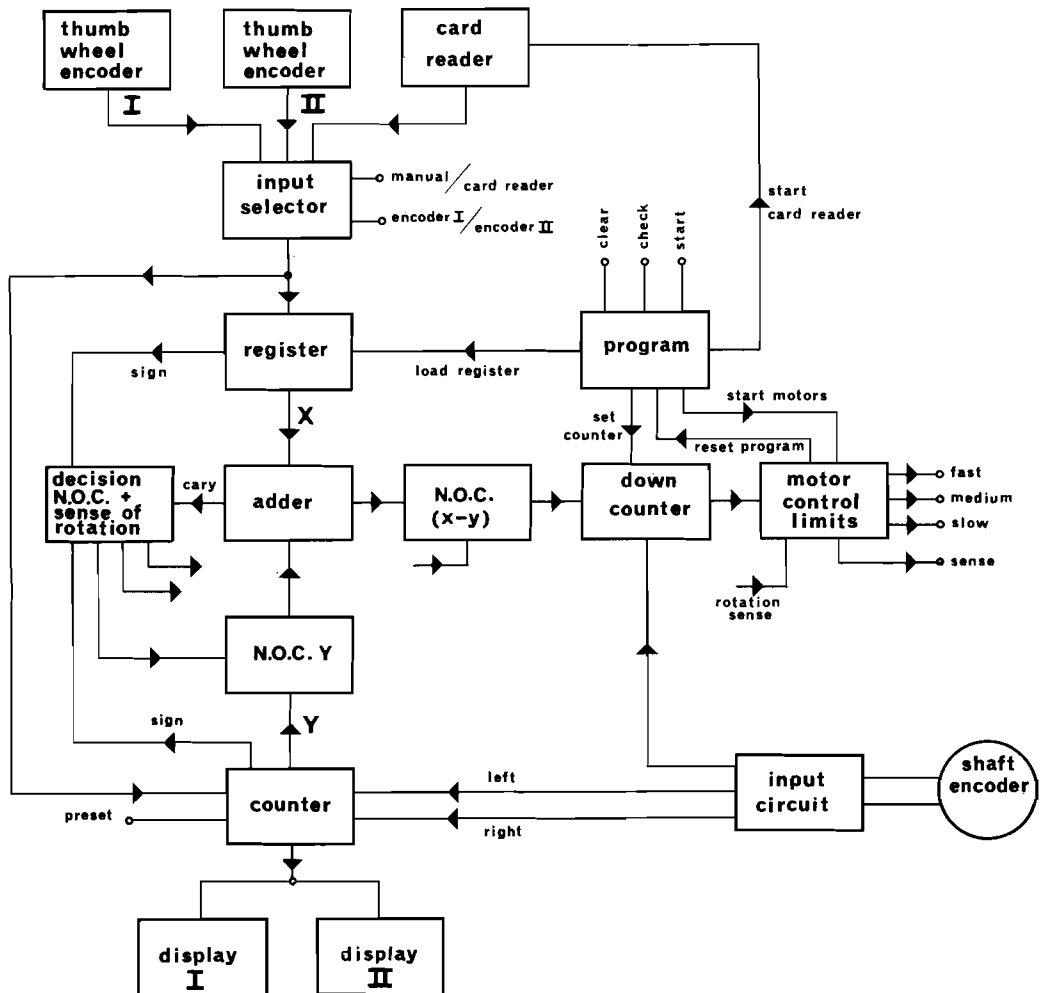


Fig. 19. Block-diagram of the positioning unit of the "mini-mount".

must be in BCD (Binary Coded Decimal) form, a set-up has been chosen, in which the data in the entire apparatus is processed bit parallel, and character parallel in BCD form. This means that the calculating part must be able to add or subtract BCD coded figures. Adding is effected with the aid of a binary full adder, followed by a decoding circuit for converting the binary result into BCD form. This decoder must contain the following conditions, as indicated in the inversion table (table 7).

Table 7

	sum		binary			sum		BCD		
	<i>d</i>	<i>c</i>	<i>b</i>	<i>a</i>		<i>D</i>	<i>C</i>	<i>B</i>	<i>A</i>	
0	0	0	0	0		0	0	0	0	
1	0	0	0	1		0	0	0	1	
⋮										
9	1	0	0	1		1	0	0	1	
10	1	0	1	0		0	0	0	0	Carry
11	1	0	1	1		0	0	0	1	Carry
⋮										
15	1	1	1	1		0	1	0	1	Carry
16	0	0	0	0	Carry	0	1	1	0	Carry
17	0	0	0	1	Carry	0	1	1	1	Carry
18	0	0	1	0	Carry	1	0	0	0	Carry
19	0	0	1	1	Carry	1	0	0	1	Carry

$$\text{Carry}_{\text{decimal}} = T = \text{Carry}_{\text{binary}} + \overline{b\bar{c}} \cdot d \cdot \overline{\text{Carry}_{\text{bin}}}$$

$$A = a$$

$$B = b \cdot \overline{T} + \bar{b} \cdot T$$

$$C = c \cdot \overline{T} + \bar{c} \cdot b \cdot T$$

$$D = d \cdot \overline{T} + \bar{d} \cdot \bar{b} \cdot \bar{c} \cdot T$$

This circuit is executed with the aid of three standard packages as indicated in Fig. 20.

Decimal subtraction corresponds to adding the decimal complement:

$$X - Y \equiv X + (10^{n+1} - Y) - 10^{n+1} \dots \dots \dots (4.3.1)$$

in which:

X and *Y* are the decimal figures which are to be subtracted from each other and *n* is the highest power of 10 in the figures *X* or *Y* (example: in the case of 357 - 24 : *n* = 2).

In electronic practice it is simpler to determine $(10^{n+1} - 1) - Y$ and, afterwards, add 1 again:

$$X - Y \equiv [X + \{(10^{n+1} - 1) - Y\} + 1] - 10^{n+1} \dots \dots \dots (4.3.2)$$

For the sake of elucidation the following numerical example is given:

$$\begin{array}{r}
 X: 456 \\
 Y: 123 - \rightarrow \{(10^{n+1}-1)-Y\}: 876 + \\
 \hline
 X - Y \quad 333
 \end{array}
 \qquad
 \begin{array}{r}
 X : 456 \\
 \rightarrow (10^{n+1}-1)-Y: 876 + \\
 \hline
 1332 \\
 \hline
 1 + \\
 \hline
 X - Y: 1333 - 10^3 = 333
 \end{array}$$

In this case in which $X > Y$ the result of $X + \{(10^{n+1}-1)-Y\}$ will always be $\geq 10^{n+1}$. This factor 10^{n+1} (the extreme left 1 (carry) in the numerical example) must be subtracted from the intermediate result (\equiv omitted). It does indicate, however, that the final result is positive and in this case this 1, is added to the Least Significant Bit (LSB). (See equation (4.3.2).

In the case of $X \leq Y$ the result of $X + \{(10^{n+1}-1)-Y\}$ will always be smaller than 10^{n+1} which means that no carry of 10^{n+1} becomes available to add to the intermediate result. This is an advantage rather than a disadvantage, as can be seen from:

$$X - Y \equiv X + (10^{n+1} - Y) - 10^{n+1} \dots \dots \dots (4.3.3)$$

$$10^{n+1} - (Y - X) \equiv X + (10^{n+1} - Y)$$

$$\{(10^{n+1} - 1) - (Y - X)\} \equiv [X + \{(10^{n+1} - 1) - Y\}] \dots \dots \dots (4.3.4)$$

a numerical example:

$$\begin{array}{r}
 X: 123 \\
 Y: 456 - \rightarrow (10^{n+1}-1)-Y: 543 + \\
 \hline
 X - Y: -333 \qquad (10^{n+1}-1)-(Y-X): 666
 \end{array}
 \qquad
 \begin{array}{r}
 X: 123 \\
 \rightarrow (10^{n+1}-1)-Y: 543 + \\
 \hline
 (10^{n+1}-1)-(Y-X): 666
 \end{array}$$

$|X - Y| = Y - X: 333 \qquad |X - Y|: 333$

The absence of the carry of 10^{n+1} indicates that $X - Y \leq 0$ and that of the intermediate result the 9's-complement must be taken again to find the correct value of $|X - Y|$.

The quantity $\{(10^{n+1}-1)-Y\}$ is obtained in the circuit by taking the 9's-complement of each Y digit separately. With the aid of a conversion table it is easy to see how this can be effected, see table 8.

Table 8

number (decimal)	number (BCD)				9-complement			
	2 ³	2 ²	2 ¹	2 ⁰	2 ³	2 ²	2 ¹	2 ⁰
	<i>d</i>	<i>c</i>	<i>b</i>	<i>a</i>	<i>D</i>	<i>C</i>	<i>B</i>	<i>A</i>
0	0	0	0	0	1	0	0	1
1	0	0	0	1	1	0	0	0
2	0	0	1	0	0	1	1	1
3	0	0	1	1	0	1	1	0
4	0	1	0	0	0	1	0	1
5	0	1	0	1	0	1	0	0
6	0	1	1	0	0	0	1	1
7	0	1	1	1	0	0	1	0
8	1	0	0	0	0	0	0	1
9	1	0	0	1	0	0	0	0

$$\begin{aligned}
 A &= \bar{a} \\
 B &= b \\
 C &= c\bar{b} + \bar{c}b \\
 D &= \bar{b}\bar{c}\bar{d}
 \end{aligned}$$

The 9-complementer must also be able to leave the input magnitudes unchanged so that, besides the conditions mentioned above an additional *OR*-condition must be built in which has to be carried out, for instance, by means of a circuit as indicated in Fig. 21.

Positioning can entail six different combinations of the *X* and *Y* values, the correct calculation of the sum or difference of which must be carried out and the correct direction of rotation must be determined for the driving-motors. See table 9.

Table 9

sign <i>X</i>	sign <i>Y</i>	<i>X</i> > <i>Y</i> <i>X</i> < <i>Y</i>	carry 10^{n+1}	N.O.C. <i>Y</i>	N.O.C. $ X - Y $	rotation sign
+	-	× ×	× ×	<i>N</i>	<i>N</i>	+
-	+	× ×	× ×	<i>N</i>	<i>N</i>	-
+	+	>	1	<i>C</i>	<i>N</i>	+
+	+	<	0	<i>C</i>	<i>C</i>	-
-	-	>	1	<i>C</i>	<i>N</i>	-
-	-	<	0	<i>C</i>	<i>C</i>	+

× × : irrelevant
 N.O.C.: Number Or Complement

For the determination of N.O.C.-*Y* the following condition holds good:

Complement as sign *X* = sign *Y* (*x* = *y*) or in circuit formula: $C = x\bar{y} + \bar{x}y$.

For the determination of N.O.C. $|X - Y|$ the following holds good:

Complement as *x* = *y* and carry $10^{n+1} = 0$ ($C_{10} = 0$) or in formula form: $C = x\bar{y} + \bar{x}y \cdot C_{10}$.

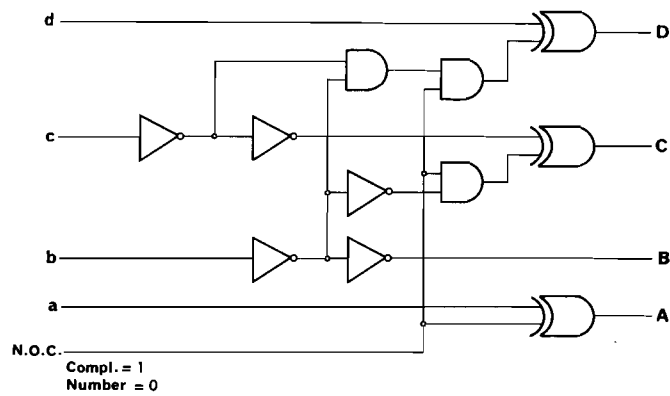


Fig. 21. Number Or Complement (N.O.C.) circuit.

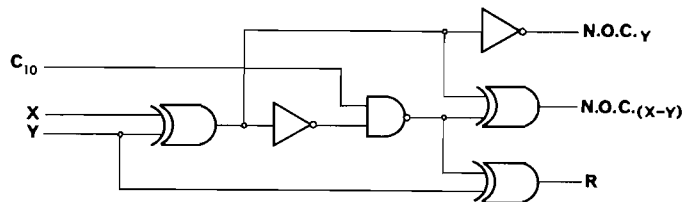


Fig. 22. Determination of N.O.C. and direction of rotation.

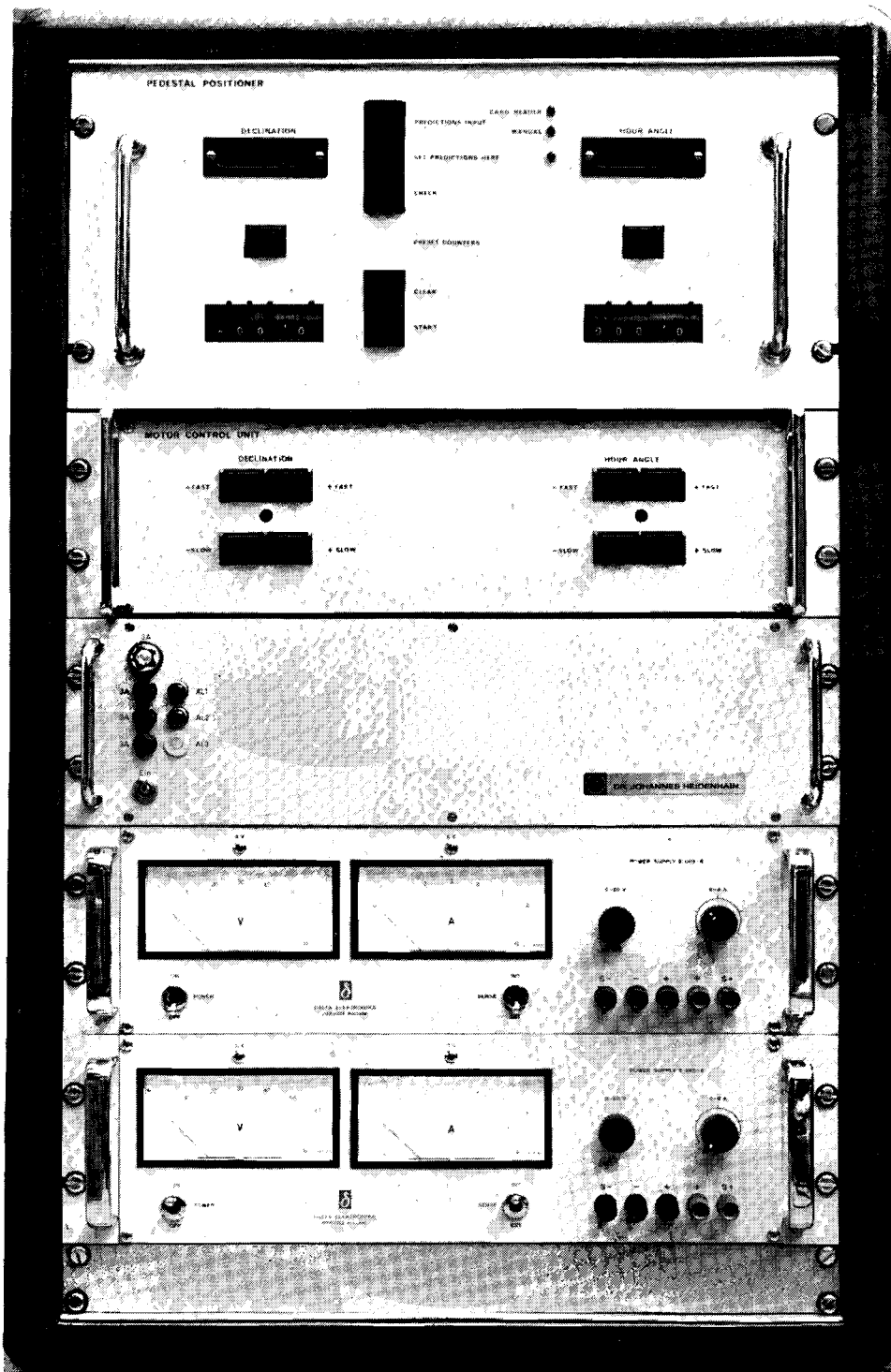


Fig. 23. Control panels of the positioning equipment.

For the determination of the direction of rotation R the following holds good:

$R = \bar{y}$ except if $x = y$ and $C_{10} = 1$

in circuit formula: $R = \overline{\{(x\bar{y} + \bar{x}y) \cdot C_{10}\}} Y + \overline{\{(x\bar{y} + \bar{x}y) \cdot C_{10}\}} \bar{y}$.

The combination of these latter three circuit formulas can lead, for example, to the circuit as indicated in Fig. 22.

c. *Motor-driving*

The mounting is driven by two 150W DC motors (disk-armature motors); the power is supplied by two stabilized supply-devices, the output voltage of which can be controlled by means of an externally connected control signal. The control signal is obtained by means of a constant speed control, which is equipped in a conventional manner with an operational amplifier which compares the desired number of revolutions with the actual number of revolutions (tacho-generator voltage). The desired speed is set by means of push-buttons (slow and fast) or by the output relays of the automatic positioning-device. For easy driving, adjustable acceleration and deceleration circuits have been provided. The maximum driving-speed amounts to approx. 220°/min so that any adjustment of the mounting can be carried out within two minutes. When more exposures have to be made during one passage of a satellite, the setting-time between the exposures is nearly always much shorter.

5 TIME-KEEPING

5.1 Time measurements

The objective of the time-measuring equipment is to relate the direction-measurements to satellites to the UTC time-scale, which has been internationally agreed upon with an accuracy which is in accordance with that of the measurement itself. This means that an absolute accuracy of 0.1 ms is sufficient. The station time-standard has been chosen so that it is not difficult to keep the station time synchronized within 10 μ s with respect to UTC. This anticipates the future use of laser-ranging equipment, for which the synchronization requirement is ten times more accurate than for the direction measurements. The registration device for relating the direction measurements to the station-time scale has been designed to give an accuracy of 0.1 ms. In Fig. 24 a block-diagram of the complete system is shown.

5.2 Time-keeping equipment

A rubidium vapor frequency standard with built-in 5 MHz to 1 pps divider chain is in use as a basis. According to the manufacturer's specifications the long-term stability must be better than $\pm 2 \times 10^{-11}$ per month. The effected calibrations indicate a considerably better stability. For calibration of the station time with respect to UTC, various methods can be applied:

- a. Rough setting of hours, minutes, seconds is effected with the aid of the public telephone time service.
- b. Exact setting of seconds is effected with the aid of time signals from the transmitter HBG (Prangins, Switzerland, 75 kHz). By means of these signals a reasonably accurate check on the correct synchronization can also be carried out. This is important for calibration method e.
- c. The frequency of the station standard is continuously checked by means of phase-comparison with respect to a standard frequency transmission in the VLF band at 60 or 75 kHz. At our location, the reception of the station MSF (Rugby, England, 60 kHz) is most stable.
- d. The ultimate calibration of the station time is done with a portable clock with respect to the time of an institute which is synchronized on an international basis with respect to UTC. In our case, this reference is the National Laboratory for calibration standards in The Hague which records the UTC time-scale with an accuracy of approx. 1 μ s (making use of a cesium standard and time comparison via, inter alia, LORAN-C).
- e. Provisions are being made for carrying out calibrations with the aid of the synchronizing pulses from a commonly received TV-transmitting station.

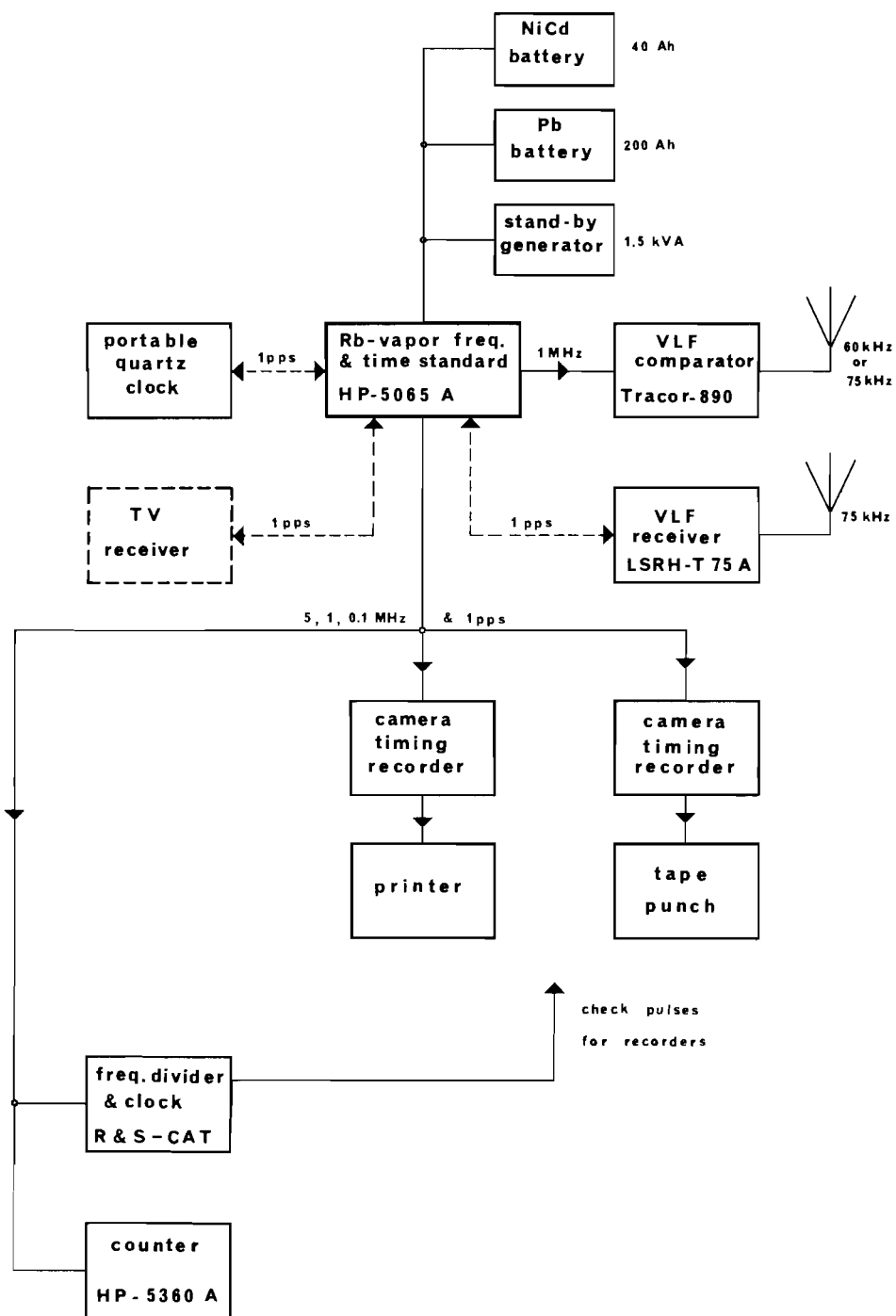


Fig. 24. Block-diagram of the total time-measuring equipment.

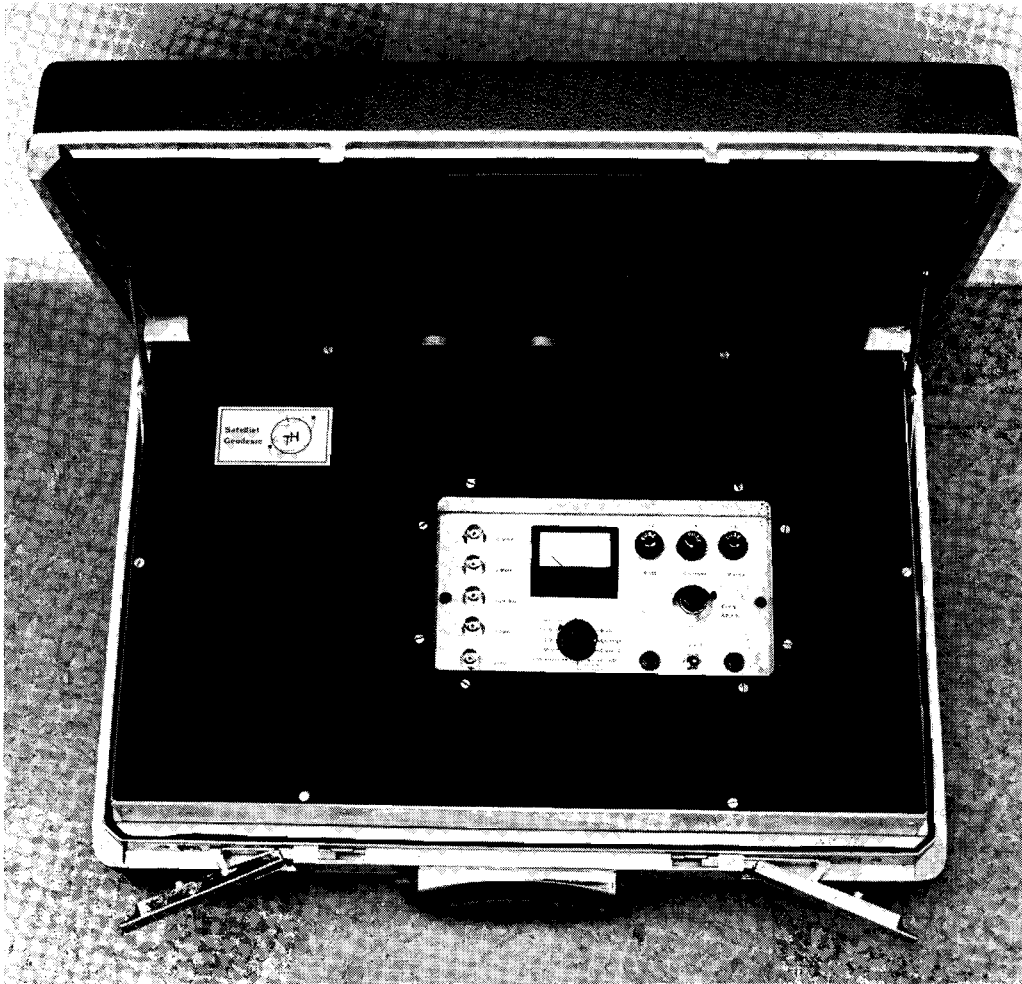


Fig. 25. Portable quartz clock.

5.3 Portable quartz clock

A portable quartz clock has been developed and constructed (see photograph, Fig. 25) for routine time-comparison. Specifications are such that, based on an accurate frequency and time-setting, no deviation greater than $5 \mu\text{s}$ is produced during a period of 3 hours. If, within this time, a return trip can be made, then an accuracy in the time comparison of approx. $1 \mu\text{s}$ can be achieved by means of interpolation. Besides this application, the instrument can serve also as a back-up station-time standard and as an accurate frequency source and time-base for various laboratory measurements.

Block-diagram (see Fig. 26)

The instrument is based on the Rohde & Schwartz type XSE quartz oscillator. This oscillator is placed in an oven, the temperature of which is controlled within 0.1°C .

The 5 MHz output signal is amplified and rectified in an input amplifier and is then

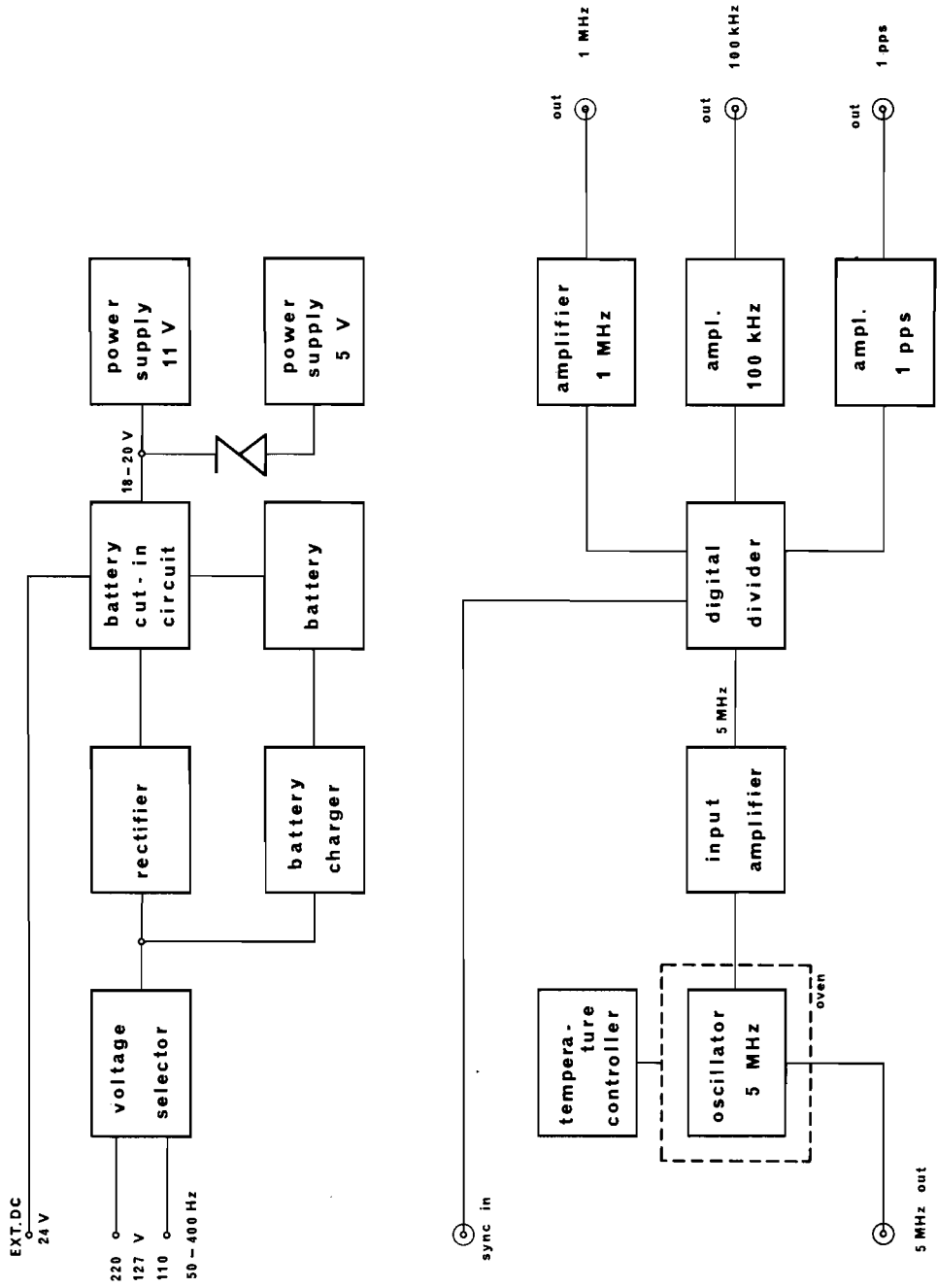


Fig. 26. Block-diagram of the portable quartz clock.

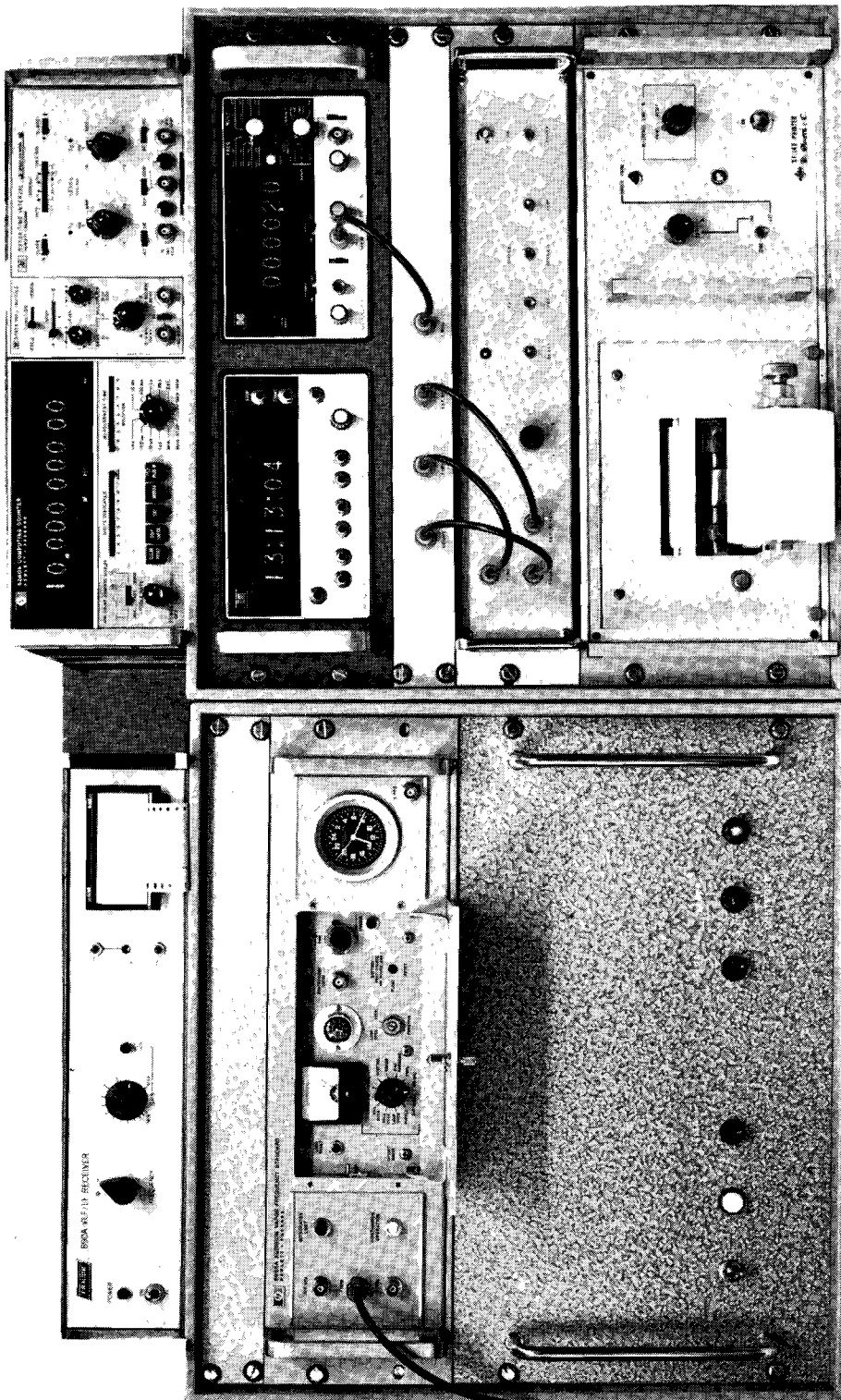


Fig. 27. Time-keeping and time-recording equipment.

supplied to a synchronous digital divider chain consisting of integrated circuits type SN 74162. The jitter of the outgoing 1 pps signal is only a few tenths of a ns. As a result of this feature it is possible to carry out rapidly – with the aid of an accurate time interval counter (e.g. the HP type 5360 A) – a very good frequency synchronization with respect to a frequency standard (readjustment to better than 1×10^{-10} within 2 minutes). This divider chain can be reset with the second signal of the reference time standard. Furthermore, a 1 MHz and a 100 kHz signal is taken from the divider chain, which signals are filtered in the relevant amplifiers.

The power for the clock is usually supplied by the mains. It may also be supplied by an external 24V DC source. If the supply voltage drops lower than 18 V, after having passed through the rectifier, then the built-in accumulator-battery is switched into circuit by the “battery cut-in circuit”. It is switched off as soon as the supply voltage is higher than 20 V.

The built-in 15-cells NiCd accumulator battery is charged by means of a charging device, which supplies a continuous charging current of 450 mA (fast charge) or 20 mA (trickle charge). Finally, the “rough” direct current is converted into voltages of 5 V and 11 V by means of two stabilized power supply devices. A moving coil meter has been fitted on the front panel for checking the correct operation and the temperature balance. By means of this meter ten vital voltages, currents and temperatures can be measured.

6 TIME RECORDERS

These units serve for recording the chopper pulses from the two cameras in the station time scale. For this purpose, two instruments have been developed which lead the registered time marks to a printer and a tape-punch. The two devices may be connected in any combination to one or both cameras.

6.1 Time recorder with printed output

Standard laboratory measuring instruments have been incorporated in the apparatus as

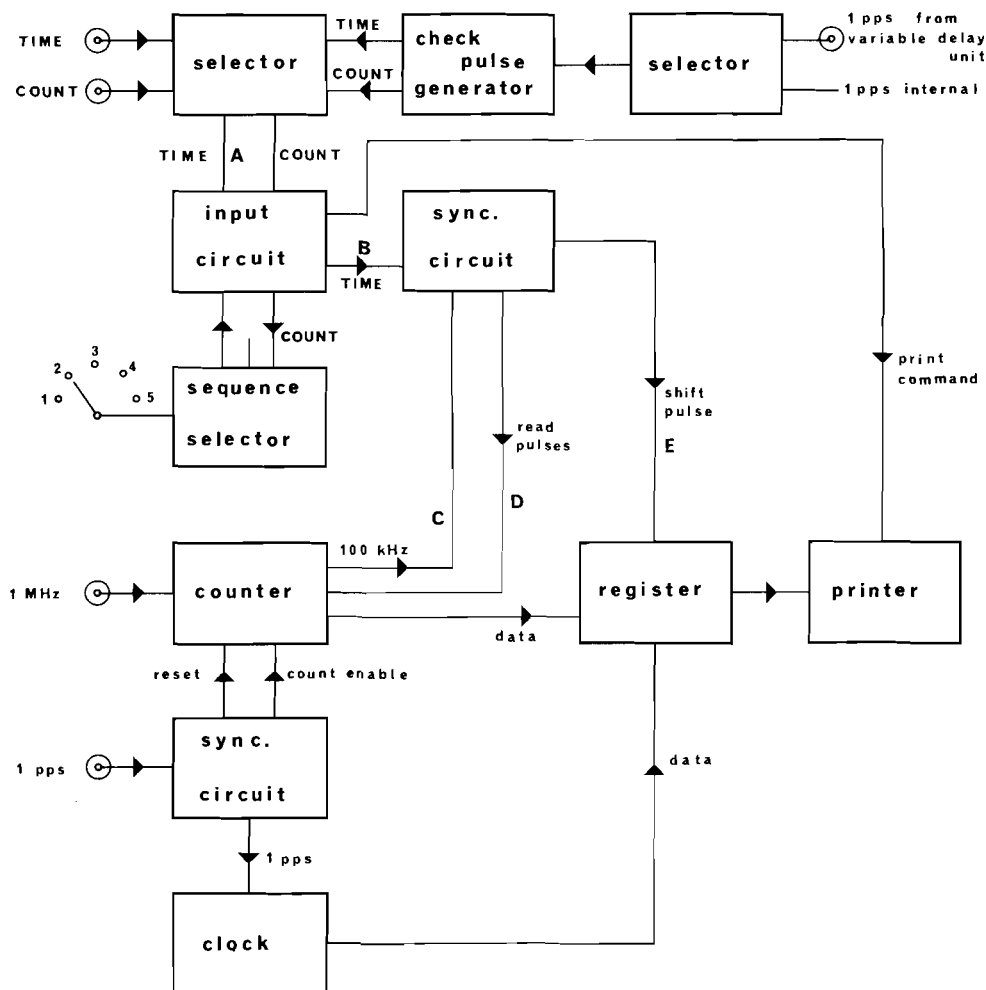


Fig. 28. Time recorder with printed output; block-diagram.

much as possible (Fig. 27). This made it possible to meet all requirements in an inexpensive way:

- accuracy of each measurement: $100 \mu\text{s}$;
- possibility of limiting the number of registered series, in accordance with a fixed cycle;
- possibility of always being able to check, in a very simple way, the reliability of the registrations.

Operation (block-diagram Fig. 28)

a. Synchronization of clock and counter

The digital clock is supplied with seconds-pulses from the station time standard. The clock should be set manually on the instrument itself. By means of the SYNC switch the counter can be synchronized with respect to the time standard, with a maximum deviation of $1 \mu\text{s}$. In pressed-in position the counter is stopped and reset with the aid of the seconds-pulses.

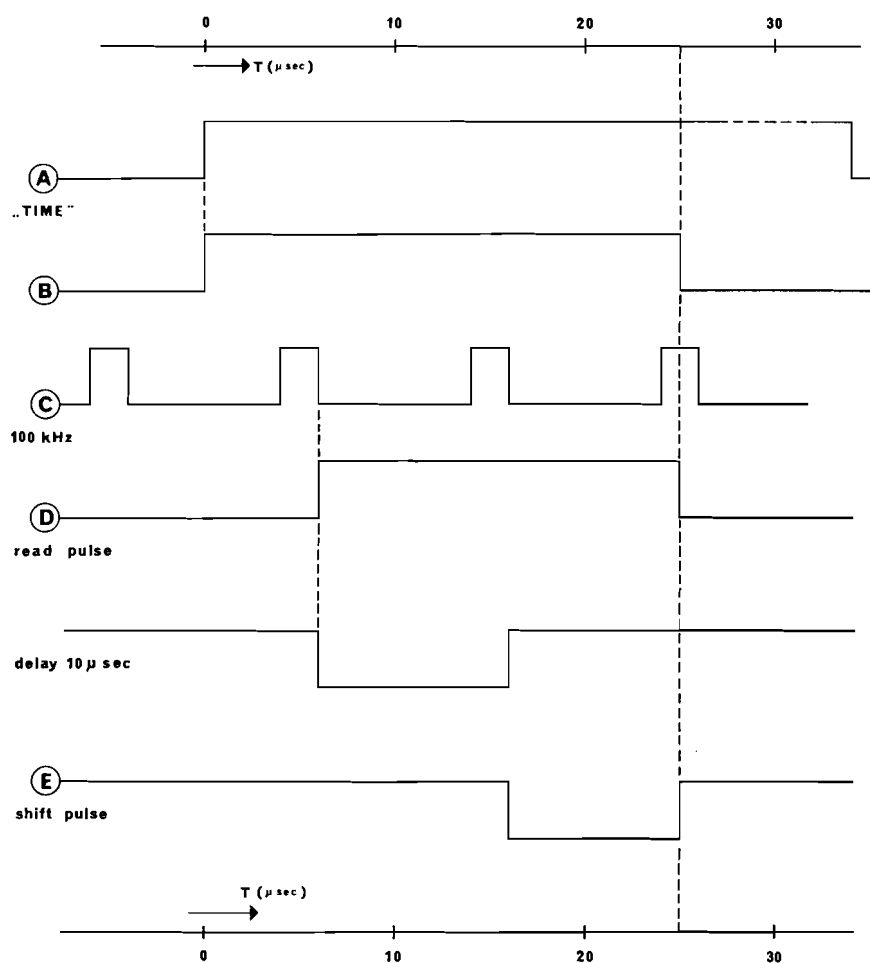


Fig. 29. Timing-diagram.

When back in the initial position the counting is resumed at the next seconds-pulse (counter in time-interval mode).

b. Processing the series of pulses to be registered

The signal entering from the cameras consists of series of four TIME pulses, followed by a COUNT pulse. These signals can be blocked in the input circuit, by means of a RESET signal from the RESET switch on the front panel or from the EXT.RESET input, or with the aid of a signal from the sequence selector described hereafter. The TIME pulses are then converted into pulses of 25 μ s width. The COUNT pulses are conveyed to the printer as PRINT COMMAND signal. In the synchronization circuit the 25 μ s wide TIME pulses are synchronized with the counting frequency of the counter (Fig. 29); this must prevent the counter from being "read out" during its so-called "ripple-time". This means that the registration of the relevant pulse may be delayed for a maximum of 10 μ s, which is negligible in view of the accuracy requirement of 100 μ s. The counter counts on the leading edge of the 2 μ s pulse (signal C); 2 μ s later the value achieved is shifted in the memory of the counter (signal D) and is kept there during the remaining part of the signal B.

After a delay of 10 μ s the shift pulse E follows, by means of which the value to be registered is taken over from the memory of the counter into the register. This procedure is repeated for the three remaining pulses of the series, after which the register is filled completely. The same procedure holds good for reading out the digital clock, differing only in that it is read out by the first pulse of the series.

The full information of the series is now available to the printer in bit parallel and character parallel form and is printed out (Fig. 30) at the next COUNT signal.

nr.	min.	sec.	$\times 10^{-4}$ sec	$\times 10^{-4}$ sec	$\times 10^{-4}$ sec	$\times 10^{-4}$ sec	check
001	9	33	1234	5678	9012	3456	B *

Fig. 30. Print-out of a series of time-recordings.

In this example a second-transfer has been carried out between the third and fourth registration, so that for the fourth registration the time recorded in seconds at the beginning of the line no longer applies. Since the TIME pulses offered do enter at almost identical intervals there is no problem. At intervals smaller than 1 second, the second-transfers can be easily recognized.

c. Checking

The construction of the register makes it necessary that four pulses be registered per series. If not, the output will be in the wrong positions of the format. For this reason the number of pulses is printed in letter-code behind the registrations. If the number is other than four, the * sign is printed in the last column and a pilot lamp on the front panel lights up. The correct operation can be checked by supplying pulses at known time-instants. The simplest way is to register by second-pulses. For this purpose a check-pulse generator has been incorporated which arranges seconds-pulses of the station time standard in series of 4, followed by a COUNT pulse. In the columns for 10^{-1} , 10^{-2} , 10^{-3} , 10^{-4} seconds, all zero's must

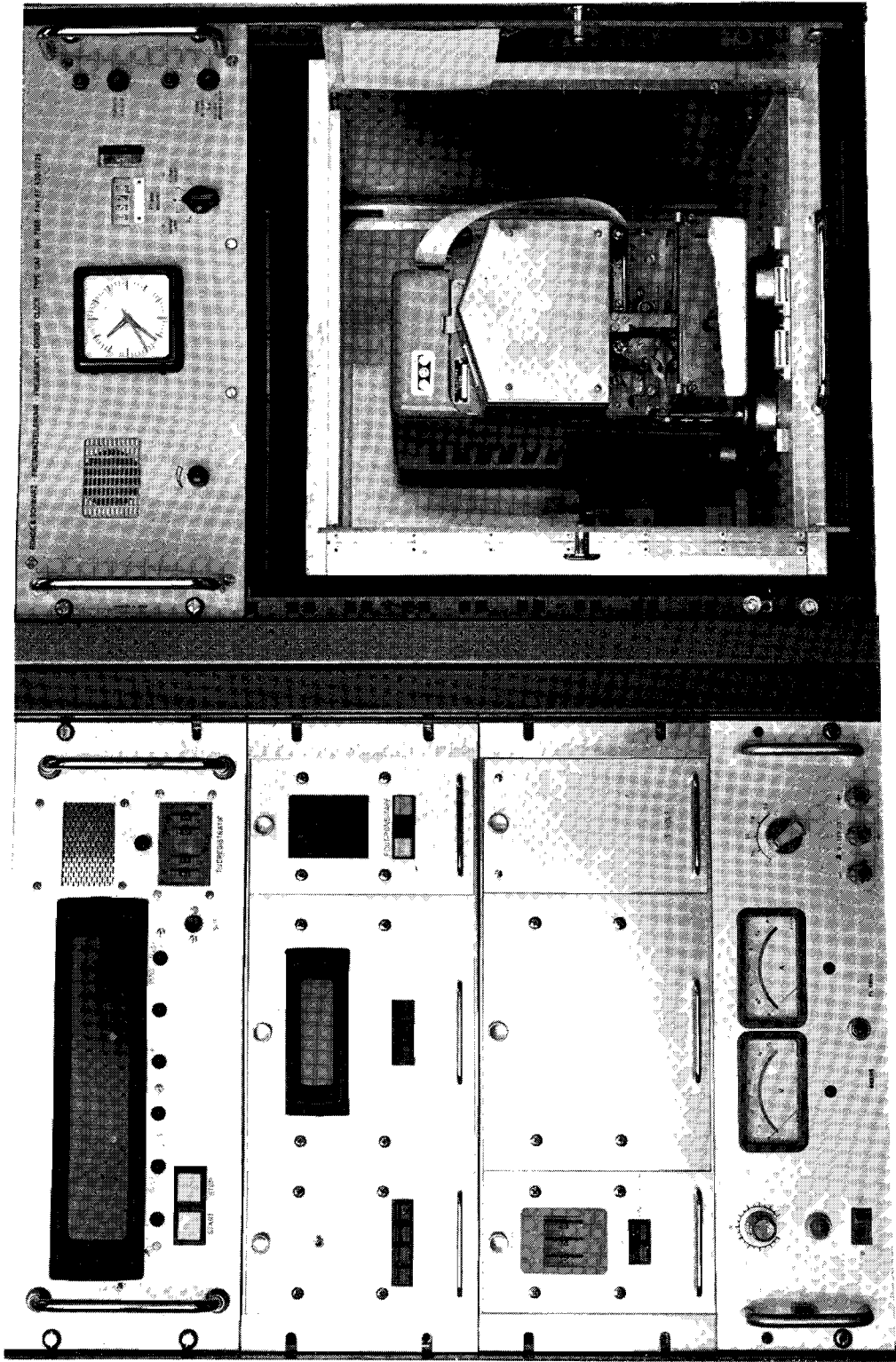


Fig. 31. Time recorder with punched tape output.

be printed. Instead of using the seconds-pulses of the time-standard, the seconds-pulses from a variable delay unit (for instance, the Rohde & Schwarz type CAT) may be supplied so that any random value can be printed out.

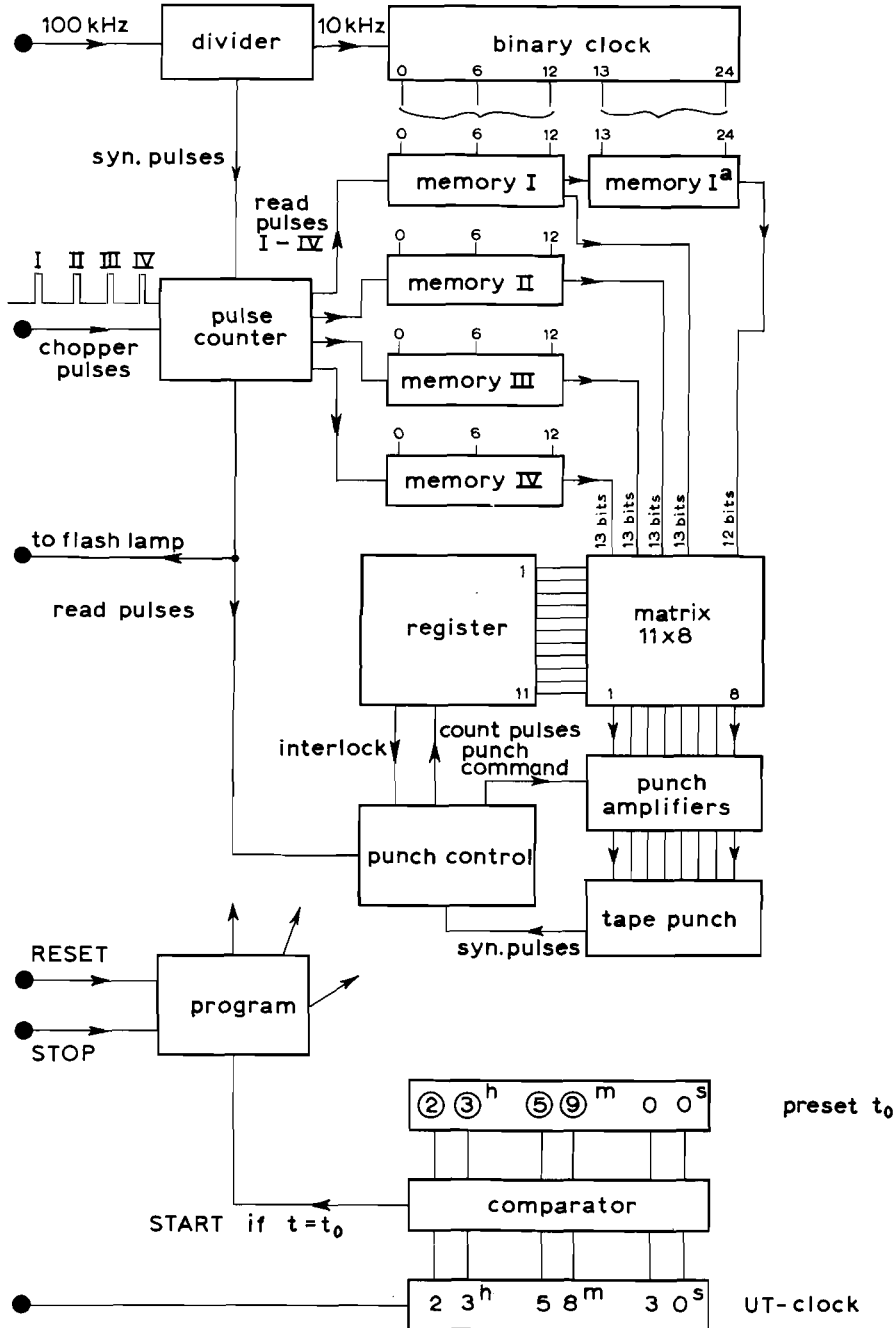


Fig. 32. Block-diagram of the time-recorder with punched output.

d. Sequence selector

The printer used here needs approximately 1 second for printing all data, after having received the PRINT COMMAND. If the repetition-frequency of the incoming measuring series is higher, series have to be omitted. By means of the selector switch on the front panel, a ratio of "series supplied to series registered" of 1, 2, 3, 4 or 5 can be set. This circuit is reset prior to starting a measurement; either automatically via the EXT.RESET input, or manually with the RESET switch. From this moment onwards the series are registered in an order of sequence, which corresponds to the multiplication table; for instance, in position 3, the series 3, 6, 9, 12 are registered.

6.2 Time recorder with punched output

A tape punch has been chosen as the output element of the second recorder (see Fig. 31), since these recordings can be processed directly in a computer. A second advantage is the high processing speed of the chopper pulses received: recording can be effected at a chopper rotation speed of 0.11 to maximum 10 rev./sec.

Operation (see block-diagram, Fig. 32)

In designing the recorder it was considered that, for the purpose of obtaining a high processing speed it was of the utmost importance that all the space on the eight hole punch-tape be used as effectively as possible. Full registration of the time marks in hours, minutes, seconds, etc. has therefore been abandoned; all data are punched also in binary form. The time-scale starts at a time instant t_0 , preset by means of thumbwheel-switches. The 100 kHz frequency from the station time standard is divided by ten first and controls, then, a binary clock, consisting of 24 flip-flops. The running-time of this clock is $2^{24} \times 10^{-4} \text{ s} \approx 28$ minutes. Input divider and binary clock are reset and started simultaneously, so that the switching-on error may not exceed 1 period of the input signal ($= 10 \mu\text{s}$), since the 100 kHz signal and the second-pulses are not in phase.

Since the chopper pulses may enter at any given moment, viz. also during the time that transfers are being effected between bits in the binary clock ($=$ ripple time), a synchronization must be made between the read-in pulses and the 10 kHz counting pulses of the binary clock. This is done in the same way as described in section 6.1b. This synchronization takes place in the pulse counter. The read-in pulses are supplied also to a flash-unit which supplies light-flashes for calibration (see section 2.4).

To prevent as much as possible the registration of unnecessary information on each of the four read-in pulses, only part of the binary clock is read into the relevant memory. The whole binary clock is read out only at the first read-in pulse (most significant bits 13 through 24, in memory Ia). The separation between the data stored in memory Ia and the memories I, II, III, IV lies between the bits 12 and 13. Every $2^{12} \times 0.1 = 409.6$ ms a transfer is effected from bit 12 to bit 13. If such a transfer has been effected between the receipt of, for instance, the read-in pulses II and III, a lower value is registered for pulse III than for pulse II. The programme applied for reading-in the punch tapes in the computer, adds automatically a 1 to value of bit 13 for the reading out of III, etc. If the pulse distance is greater than 409.6 ms, then two transfers may have taken place and the foregoing no longer holds good.

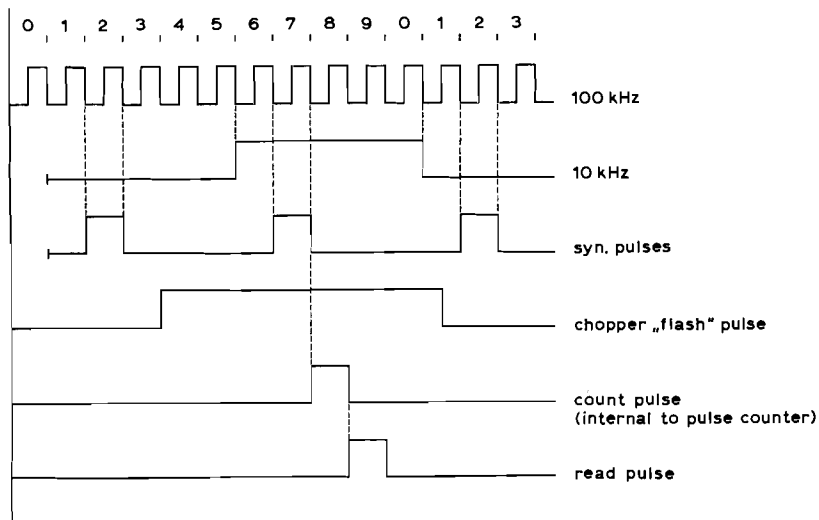


Fig. 33. Timing-diagram.

The minimum measuring speed is thus determined at one revolution of the chopper per approx. 9 seconds. The contents of the memories are distributed in a matrix, from which the data are issued to the 8 channels of the tape punch in 11 phases. The rate of data supply must be matched to the speed of operation of the tape punch. For this purpose, the tape punch transmits synchronization pulses, which are used as COUNT PULSE for the register and as PUNCH COMMAND for the punch-amplifiers. These synchronization pulses are permitted to pass if punch-work has to be done and punching is done only if a chopper pulse has entered (Fig. 33).

When the first chopper pulse has entered, the data in the corresponding first lines of the matrix are punched out. Then the punching is stopped until the second chopper pulse has entered. The same procedure takes place with the next pulses. In the lapse of time between the first of a sequence of chopper pulses and the first of the next sequence, the tape punch must punch out 11 lines. At a maximum speed of 110 lines per second, this means an upper limit to the measuring speed of 10 sequences per second. When the minimum or the maximum measuring speed is exceeded, pilot lamps on the control panel light up. If the number of incoming chopper pulses arrived is not equal to four, the registration of this sequence is unreliable. A special indication is then added to the punched format.

7 ANNEXES

7.1 Some tables with relation to the TA-120 chopper

a. The relation between $\{m_s(\max) - m_s\}$ and q

Table 10

$\{m_s(\max) - m_s\}$	q	$\{m_s(\max) - m_s\}$	q
0.0	0.00		
0.1	0.10	2.1	0.81
0.2	0.20	2.2	0.82
0.3	0.25	2.3	0.83
0.4	0.30	2.4	0.84
0.5	0.35	2.5	0.85
0.6	0.40	2.6	0.86
0.7	0.43	2.7	0.87
0.8	0.50	2.8	0.88
0.9	0.53	2.9	0.88
1.0	0.57	3.0	0.89
1.1	0.63	3.1	0.90
1.2	0.65	3.2	0.90
1.3	0.68	3.3	0.91
1.4	0.70	3.4	0.91
1.5	0.72	3.5	0.92
1.6	0.73	3.6	0.92
1.7	0.75	3.7	0.92
1.8	0.76	3.8	0.93
1.9	0.78	3.9	0.93
2.0	0.80	4.0	0.93

When participating in an international project the satellite predictions are calculated centrally in most cases, and then are conveyed (e.g. per telex). The predictions are of a general character; in most cases they contain a minimum of data. Let us assume that, besides the camera settings, the following data are given: ω and m_s . From the tracking power P , (2.3.3) then yields $m_s(\max)$ and from $\{m_s(\max) - m_s\}$, q results from table 10. With q and ω the nomogram in Annex 7.2 can be used in order to find the number of revolutions t to be set. This may also be calculated by means of a computer; the tables and the nomogram are necessary, however, if no computer is available, and further in all cases, where the predictions become available only just before the time of observation (in the evening, at night, week-end).

b. Some interval and cycling-times for various speeds (for TA-120)

(2.4.15) yields:

$$t = 60\omega \frac{(1750q + 875)}{L_{\text{bpt}}} \dots \dots \dots (7.1.1)$$

With the same ω , different values of t can be found, dependent on the satellite speed and the desired length of the satellite image.

For instance, with $\omega = 0.87^\circ/s$ and $L_{bpt} = 70 \mu m$:

Table 11

q	t
0.0	660
0.1	790
0.2	920
0.3	1050
0.4	1180
0.5	1310
0.6	1440
0.7	1580
0.8	1710
0.9	1840
1.0	1970

Table 12

L_{bpt}	t
30	3050
40	2280
50	1830
60	1520
70	1310
80	1140
90	1020
100	910

or, with $\omega = 0.97^\circ/s$, $q = 0.5$:

Practice has shown that an average good picture made with the TA-120 camera has approximately 32 measurable satellite image points. This means that the intercepting strip has rotated 32 times; during this procedure the circumference of the driving belts (= 42 cm) has been covered 32 times. Assuming that approximately $4^\circ.5$ of the field of view is used, and that the satellite image passes this $4^\circ.5$ with an angular speed ω , then the average linear speed of the strip at this specific ω can be computed. Taking this as a basis, the following table can be given:

Table 13

h km	ω°/s	T	t_o ms	t_i ms
500	0.872	21.36	162	8.3
1000	0.421	10.38	334	17.1
1500	0.272	6.74	515	26.4
2000	0.198	4.89	709	36.3
2500	0.154	3.80	913	46.7
3000	0.124	3.06	1135	58.1
3500	0.104	2.56	1354	69.4
4000	0.089	2.20	1578	80.8
4500	0.077	1.90	1826	93.5
5000	0.068	1.68	2069	105.9
5500	0.060	1.48	2346	120.1
6000	0.054	1.33	2608	133.5
7000	0.045	1.11	3134	160.4
8000	0.038	0.94	3684	188.6
9000	0.033	0.82	4242	217.2
10000	0.028	0.69	5000	256.0

in which:

h = height of satellite

ω = topocentric angular-speed of the satellite in the field of view, when passing the zenith

T = number of revolutions per second of the sprockets
 t_o = cycling-time of the strip
 t_i = interval time

The above-mentioned numerical values may also be calculated from (7.1.1), if the following is taken:

$$\frac{1750q + 875}{L_{bpt}} = 24.5 \quad \dots \dots \dots (7.1.2)$$

From (7.1.1) and (7.1.2) it follows that a reasonable approach for (7.1.1) may be:

$$t = 60 \times 24.5 \times \omega$$

or

$$T = 24.5 \times \omega \quad \dots \dots \dots (7.1.3)$$

A still better approximation may be found by taking that for a specific satellite:

$$\omega = \frac{C}{A} \quad \dots \dots \dots (7.1.4)$$

in which:

C = an arbitrary constant
 A = the distance to the satellite

From (7.1.3) and (7.1.4) it finally follows that:

$$t = \frac{C'}{A} \quad \dots \dots \dots (7.1.5)$$

or:

$$T = \frac{C''}{A}$$

in which:

$$C' = 1470C$$

and

$$C'' = 24.5 C$$

When the relation between speed of the chopper and the voltage of the power supply device is known, the voltage to be set for the supply of the chopper motor to be used, follows quite straightforwardly from (7.1.5) taking account of the distance to the satellite.

7.2 Nomogram "revolutions per minute" of the chopper motor

See Fig. 34.

7.3 Calibration

a. The direction to the centre of the satellite image point

In Fig. 35 β is the "image plane" and Ω is the plane in which the chopping strip moves. The two planes are parallel to the plane through the centre of the objective (containing A , B and D).

ω %sec

NOMOGRAM rpm chopper-motor

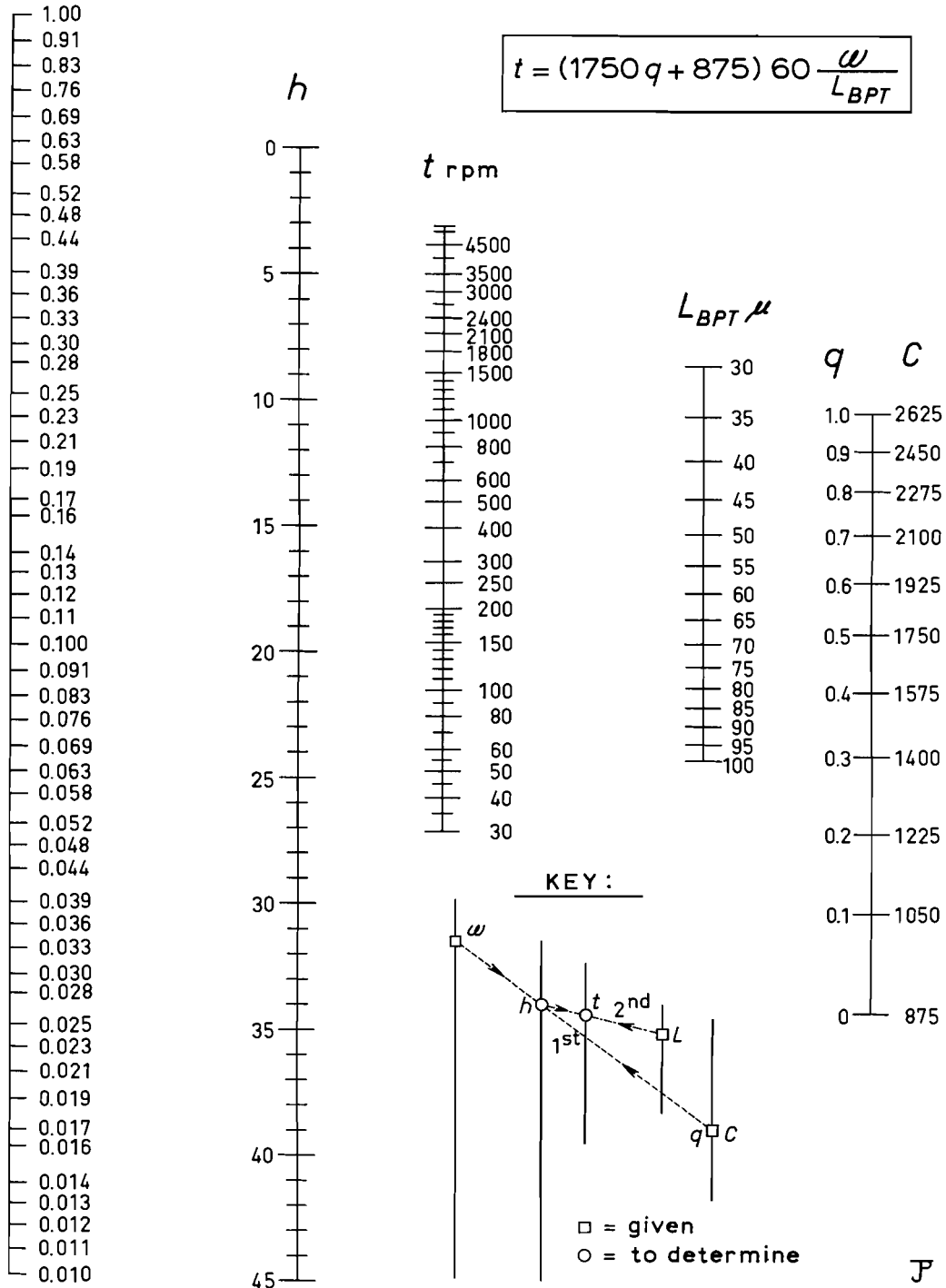


Fig. 34. Nomogram number of revolutions of chopper motor.

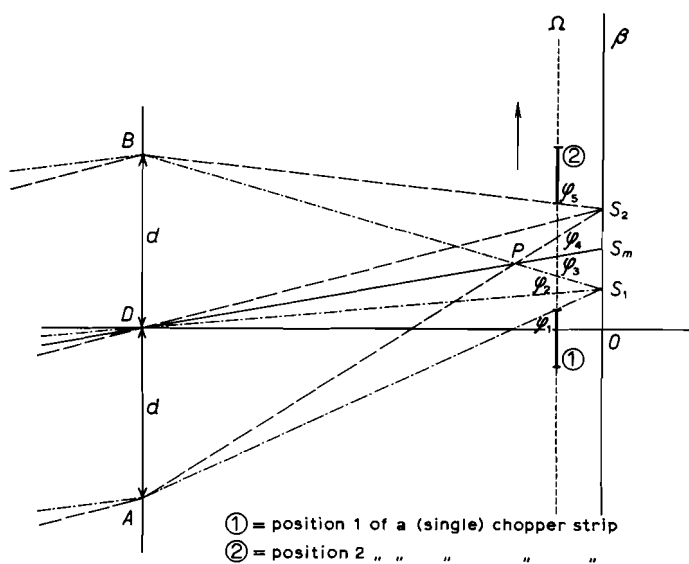


Fig. 35. A single chopper strip moving in front of the image plane.

S_1 is the position of the satellite image at the moment the strip (which moves in the direction of the arrow, just like the satellite image) starts suppressing the light beam; S_2 is the position of the satellite image at the moment that the strip releases the light beam completely again. From the figure it can be seen that if $S_1 S_m = S_2 S_m$, i.e. if we consider the centre of an interception, from the congruence of a number of triangles it follows: $Q_1 Q_3 = Q_3 Q_5$. So Q_3 lies on DS_m . If we assume that both the strip and the satellite image maintain a constant speed (which is approximately the case), it will be clear that at every centre of an interception, the position of the strip is such that its centre is cut by the line (direction) from D to the middle of the interception. In the case where a double strip is used, an analogous proof can be given.

Conclusion

The direction to the centre of each satellite image point always contains the “centre of the strip”, at the moment it is produced.

b. Calibration with the aid of diffused light

In Fig. 36, M'_3 has been assumed to be the centre of an interception; the corresponding position of the strip $S_1 S_2$ has been indicated. Diffused light enters, shadow and half-shadows have been indicated.

Congruence proves that:

$$\left. \begin{aligned} S'_1 &= \frac{1}{2}(S''_1 + S'''_1) \\ S'_2 &= \frac{1}{2}(S''_2 + S'''_2) \end{aligned} \right\} \dots \dots \dots (7.3.1)$$

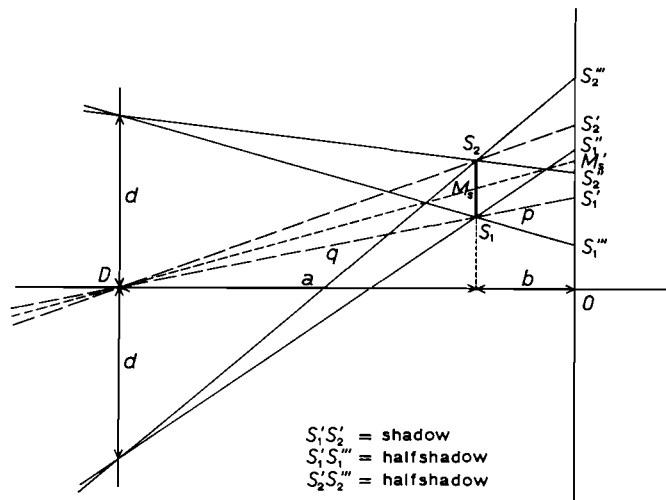


Fig. 36. Configuration showing shadows of a single strip during calibration.

Now:

$$\frac{S_1''S_1'}{p} = \frac{d}{q}$$

and:

$$\frac{p}{q} = \frac{a}{b}$$

so that:

$$S_1''S_1' = \frac{d}{b} a$$

moreover:

$$S_2''S_2' = \frac{d}{b} a$$

so that:

$$S_1''S_1' = S_2''S_2' \dots \dots \dots (7.3.2)$$

From (7.3.2) and (7.3.1) it follows that:

$$S_2'S_2''' = S_1'S_1''' \dots \dots \dots (7.3.3)$$

Because congruence also shows that:

$$S_1'M'_s = S_2'M'_s \dots \dots \dots (7.3.4)$$

(7.3.3) and (7.3.4) mean:

$$S_1'''M'_s = S_2'''M'_s$$

This shows that, when diffused light is used, in every position of the strip, the centre of an interception coincides with the centre of the shadow. When a double strip is used, an analogous proof can be given.

Conclusion

In any position of the double strip the centre of a satellite image coincides with the centre of the shadow which is formed when diffused light enters. Therefore during the calibration procedure, no corrections need be made to the calibration coordinates of the satellite image points and calibration lines.

7.4 Basic design data for the K50-chopper

Table 14

h km	ω°/s	T	t_0 ms	t_i ms
500	0.872	10.01	415	23.5
1000	0.421	4.83	859	48.7
1500	0.272	3.12	1333	75.5
2000	0.198	2.28	1830	103.6
2500	0.154	1.76	2355	133.3
3000	0.124	1.42	2920	165.3
3500	0.104	1.19	3486	197.4
4000	0.089	1.02	4076	230.8
4500	0.077	0.88	4711	266.7
5000	0.068	0.78	5326	301.5
5500	0.060	0.69	6057	342.9
6000	0.054	0.62	6708	379.7
7000	0.045	0.52	8030	454.5
8000	0.038	0.44	9549	540.5
9000	0.033	0.38	11041	625.0
10000	0.028	0.32	12926	731.7
	0.020	0.23	18275	1034.5

The table for the values $\{m_{s(\max)} - m_s\}$ is almost (within the precision required) the same as for the TA-120.